PRESSURE DROP AND HEAT TRANSFER FOR LIQUID-LIQUID DISPERSIONS IN TURBULENT FLOW IN A CIRCULAR TUBE

by

CHARLES HARRY WRIGHT

A THESIS

submitted to

OREGON STATE COLLEGE

in partial fulfillment of
the requirements for the
degree of

MASTER OF SCIENCE

June 1960

APPROVED:

Redacted for Privacy

Professor of Chemical Engineering

In Charge of Major

Redacted for Privacy

Head of Department of Chemical Engineering

Redacted for Privacy

Chairman of School Graduate Committee

Redacted for Privacy

Dean of Graduate School

Redacted for Privacy

Date thesis is presented

Typed by Barbara Wright

ACKNOWLEDGMENTS

The writer is priviledged to make the following acknowledgments:

To the National Science Foundation for the financial support in the form of a research grant.

To Dr. James G. Knudsen, the author's major professor, for outlining the general problem and the type of equipment which would be required, for obtaining the research grant, and for the helpful guidance during the course of the work.

To John A. Cengel, graduate student in Chemical Engineering, for helping in the construction of the apparatus which was used for both investigations.

Finally to my wife Barbara, who took care of our child, maintained our household and typed this thesis, and to whom this thesis is dedicated.

TABLE OF CONTENTS

TABLE OF CONTENTS (continued)

LIST OF FIGURES

LIST OF TABLES

PRESSURE DROP AND HEAT TRANSFER FOR LIQUID-LIQUID DISPERSIONS IN TURBULENT FLOW IN A CIRCULAR TUBE

CHAPTER 1

INTRODUCTION

For many years investigators have been studying the flow behavior of single-phase fluids. Only recently has attention been brought to the problems involved in two-phase systems. The design of modern fluidized catalytic reactors and the problems of liquid-liquid extraction have prompted much work in this field.

The types of two-phase systems are liquid-vapor, liquid-liquid, liquid-solid, and vapor-solid mixtures. All of the above types have been studied by investigators and the work has also been extended to three-phase systems. Much of the work has been done to evaluate the properties of the systems under flow conditions.

Information on the various properties of a two-phase system is necessary to solve the problems encountered in industry. This is apparent when one considers that pumping power requirements are directly dependent on the frictional pressure losses; flow behavior is important when the problem of measuring flow rates is considered; and heat transfer characteristics are necessary in the design of many pipe-line reactors.

The present work is concerned with heat transfer to

a liquid-liquid dispersion in turbulent flow in a circular tube. Equipment was designed to measure film heat transfer coefficients and also the friction factor for turbulent flow. The friction factor measurements were necessary to evaluate some of the properties of the dispersion under flow conditions. This thesis presents the experimental results of this investigation.

CHAPTER 2

LITERATURE SURVEY AND THEORETICAL BACKGROUND

General Review

The need for experimental work in two-phase flow has increased greatly during the past several years due to the conversion of many batch processes to continuous or flow processes. The use of the fluidized bed has demonstrated the need for considerable work in gas-solid, gas-liquid, liquid-solid, and liquid-liquid systems.

There has been extensive investigation of gas-solid, gas-liquid, and liquid-solid systems. Relatively little work has been reported on liquid-liquid systems. This review will be confined to a consideration of work done on solid-liquid and liquid-liquid systems since these two-phase systems have similar characteristics. The bulk of the literature covered deals with turbulent flow in tubes.

Early work on friction losses was done by Dix and Blair (12, p. 574) and Caldwell and Babbitt (7, p. 257) on suspensions of muds and sludges. Due to the non-Newtonian characteristics of these suspensions, Alves, Boucher, and Pigford (1, p. 388) developed relations by which the properties of these suspensions could be accounted for in the design of pipe lines. Recently work has been done on the heat transfer characteristics of water slurries of chalk,

sand, and several metals by Bonilla, Cervi, Colven, and Wang (5, p. 127), Orr and DallaValle (28, p. 29), Salamone and Newman (32, p. 283), and Miller and Moulton (25, p. 15).

The flow characteristics of an oil-water mixture were investigated by Russell, Hodgson, and Govier (39, p. 9) and the thermal conductivity of several liquid-liquid emulsions was measured by Wang and Knudsen (43, p. 1667). Considerable work has been done on the viscosity of emulsions and suspensions and numerous equations have been developed to extend the theoretical equation of Einstein.

Heat Transfer - General

There are several types of heat transfer but the only type to be considered in the following work will be forced convection during turbulent flow in tubes. Reynolds (18) proposed the following equation for the transfer of heat through a pipe-wall to water following through the pipe.

$$h = \alpha \frac{C_p \mu}{D} \left(\frac{DG}{\mu}\right) \tag{1}$$

where

h = heat transfer coefficient = $q/A(t_w - t_b)$

Cp = heat capacity

μ = viscosity

D = inside diameter of pipe

G = mass velocity in pipe

ρ = density of flowing fluid

n and α are constants

This equation was tested by Stanton and Pannell (40, p. 119); Boussinesq (6) derived an equation by dimensional analysis which fairly well substantiated the previous work by Stanton and Reynolds.

$$h = \frac{k}{D}\phi\left(\frac{DV\rho}{\mu}\right)\psi\left(\frac{C_p\mu}{k}\right) \tag{2}$$

Independently Nusselt (33, p. 736) derived the equation

$$h = \frac{\alpha_2 k}{D}\left(\frac{DV\rho C_p}{k}\right)^n \tag{3}$$

and applied it to his data. He obtained a value of n = 0.785 for water. Grober (22, p. 234) later proposed a similar equation for liquids and gases.

Heat transfer data for water and several oils were measured by Morris and Whitman (26, p. 234). Their data was fairly well correlated by plotting $\left(\frac{hD}{k}\right)/\left(\frac{C_p\mu}{k}\right)^{0.37}$ vs. $(DV\rho/\mu)$ for the heating of the liquids by steam.

Using the data of Morris and Whitman (26, p. 234) McAdams and Frost (22, p. 234, 23, p. 323) Dittus and Boelter (11, p. 443) plotted the data in the form of the

following relation.

$$\frac{hD}{k} = f\left(\frac{GD}{\mu}\right) \cdot \left(\frac{C_p\mu}{k}\right) \tag{4}$$

and obtained the equation

$$\frac{U'D}{k} = 19.5\left(\frac{DG}{\mu}\right)^{0.8}\left(\frac{C_p\mu}{k}\right)^{n} \tag{5}$$

where n = 0.3 for cooling and 0.4 for heating

U' = overall heat transfer coefficient.

The basic equation of Nusselt

$$\frac{hD}{k} = a\left(\frac{DV\rho}{\mu}\right)^{n}\left(\frac{C_p\mu}{k}\right)^{m} \tag{6}$$

was modified by Sherwood and Petrie (33, p. 736) Smith (37, p. 83) and several other investigators and finally resulted in the general equation:

$$\frac{hD}{k} = 0.023\left(\frac{DV\rho}{\mu}\right)^{0.8}\left(\frac{C_p\mu}{k}\right)^{n} \tag{7}$$

where

n = 0.3 for cooling

n = 0.4 for heating.

The equation is generally attributed to Dittus and Boelter for the flow of single phase fluids in pipes.

Colburn (10, p. 174) attempted to correlate forced convection heat transfer data and compared it with fluid friction. The two exponents on the Prandtl number could

be eliminated by considering the properties of the fluid at the film temperature. The film temperature was defined as the average temperature of the laminar layer of the fluid at the pipe wall and it was evaluated by averaging the bulk temperature and the wall temperature:

(8) $$t_f = t_b + \tfrac{1}{2}(t_w - t_b)$$

where

t_f = film temperature

t_b = bulk temperature

t_w = wall temperature.

Colburn also related heat transfer data to pressure drop data by a j-factor:

(9) $$j = \tfrac{1}{2}f = \frac{h}{C_p G}\left(\frac{C_p \mu}{k}\right)^{2/3}$$

where

f = Fanning friction factor

G = mass velocity

which gave a good correlation for the available data. The present form of Colburn's equation:

(10) $$j = \frac{h}{C_p G}\left(\frac{C_p \mu_f}{k}\right)^{2/3} = 0.023\left(\frac{DG}{\mu_f}\right)^{-0.2}$$

eliminates the variable exponent in Equation (7).

In later work the effect of difference between the viscosity at the bulk temperature and wall temperature was used to make Equation (7) more universal. Sieder and Tate (34, p. 1429) added a viscosity correction factor which gave a better correlation for the various fluids considered.

$$(11) \qquad \left(\frac{h}{GC_p}\right)_b \left(\frac{C_p\mu}{k}\right)_b \left(\frac{\mu_w}{\mu_b}\right)^{0.14} = 0.023\left(\frac{DG}{\mu}\right)_b^{-0.2}$$

where

μ_w = viscosity of wall temperature

μ_b = viscosity at bulk temperature

Several investigators have attempted to derive theoretical equations to predict heat transfer rates and the temperature distribution across the tube during turbulent heat transfer. Beckers (4, p. 147) and Sleicher and Tribus (36, p. 789) derived purely mathematical formulae to predict the heat transfer and temperature distribution for the turbulent flow of a fluid in a circular tube. Sleicher presented tables of the first three eigenvalues and constants for the problem of heat flow to a constant property fluid in established turbulent flow in a round pipe for all important values of Reynolds and Prandtl moduli. The theoretical equation by Beckers agrees satisfactorily with the experimental data summarized by

Equation (7) for cooling.

Heat Transfer to a Two-Phase Fluid

The pioneering work done by Winding, Dittman, and Kranich on slightly non-Newtonian synthetic rubber latices (14, p. 125) was correlated by Equation (7). Only about one-half of their data fell within ± 10% of the equation and several points deviated as much as 35% from the correlating line. The investigators found that the suspension was pseudoplastic at the lower flow rates and behaved as a Newtonian fluid at high flow rates. The same correlating equation was used by several other investigators on suspensions of coal in water, calcium carbonate in water, graphite in water, and graphite in kerosene. Several of these systems were appreciably non-Newtonian and the apparent viscosities were calculated from pressure drop data. Miller and Moulton (25, p. 15) correlated their data on graphite in water and graphite in kerosene by the equation:

$$\frac{h_i D}{k_c} = 0.029 \left(\frac{DG}{\mu}\right)^{0.8} \left(\frac{C_{pm}\mu}{k_c}\right)^{0.4} \tag{12}$$

where the thermal conductivity of the continuous phase, the specific heat of the mixture, and apparent viscosities were used. He also correlated the data of several other authors on coal in water and calcium carbonate in water

within 15 per cent by his equation.

Orr and DallaValle (28, p. 29) made a rather extensive study of the variables in the heat transfer equation. Tareef (28, p. 29) formulated a relationship for the thermal conductivity of a two-phase system based on the properties of the constituents and their concentrations. He reasoned that the thermal field in a two-phase system was entirely analogous to the electrical field in a similar system. The following equations were then worked out for thermal field by subsequent investigators.

$$k_s = k_1 \left[\frac{2k_1 + k_p - 2x_v\ (k_1 - k_p)}{2k_1 + k_p + x_v\ (k_1 - k_p)} \right] \tag{13}$$

where

k_s, k_1, k_p = thermal conductivity of suspension, liquid, and particles respectively.

x_v = weight fraction of dispersed phase.

This equation was satisfactorily used for suspensions of powdered copper, graphite, and glass beads in water. Orr and DallaValle concluded that the thermal conductivity was independent of the degree of dispersion to a first approximation.

A viscosity correlation was obtained by Orr and DallaValle using an equation which gave very inaccurate results.

(14) $$\mu_s = \frac{1}{\left[1 - \frac{X_v}{X_{vb}}\right]^{1.8}}$$

where

μ_s = viscosity of the suspension

μ_l = viscosity of the liquid

X_v = volume fraction solids

X_{vb} = volume fraction solids in sedimented bed

The data was correlated by the above equation to ± 15% at X_v/X_{vb} equal 0.2 and ± 85% at X_v/X_{vb} equal 0.6. This equation was not recommended for pipe-line design and investigators used experimentally determined viscosities.

Their heat transfer data was satisfactorily correlated by Equation (10) using the properties evaluated at the film temperature and the volume fraction for calculating the density and the weight fraction for calculating the specific heat. The data was also correlated by the equation of Sieder and Tate:

(15) $$\frac{hD}{k_s} = 0.027\left(\frac{DV\rho_s}{\mu_s}\right)^{0.8}\left(\frac{C_{ps}\mu_s}{k_s}\right)^{1/3}\left(\frac{\mu_l}{\mu_{lw}}\right)^{0.14}$$

with the physical properties evaluated by the previously mentioned correlations. The data was well correlated by this equation for Reynolds numbers above 10,000. Good

results were obtained down to Re = 3000 but were not considered reliable. The maximum deviation of their data was of the order of ± 30%.

Salamone and Newman (32, p. 283) recommended the correlation:

$$\frac{hD}{k_l} = 0.131\left(\frac{DV\rho_s}{\mu_s}\right)^{0.62}\left(\frac{(C_{pl})\mu_s}{k_l}\right)^{0.72} \tag{16}$$

$$\left(\frac{k_s}{k_l}\right)^{0.05}\left(\frac{D}{d_p}\right)^{0.05}\left(\frac{(C_{ps})}{(C_{pl})}\right)^{0.35}$$

where subscripts

s = solution

l = liquid

p = particle

on the basis of their experimental work on suspensions of copper, carbon, chalk, and silica in water and the experimental data of previous investigators. Their work had an overall accuracy of about ± 10% and their experimental data were within this range.

Metzner, Vaughan, and Houghton (24, p. 92) obtained data for a sodium carboxymethylcellulose solution. They developed a method of determining the apparent viscosity by equating the Newtonian Reynolds number to be a generalized one as follows:

if

(17) $$\frac{DV\rho}{\mu_a} = \frac{D^{n'}V^{2-n'}\rho}{\gamma}$$

then

$$\mu_a = \gamma\left(\frac{V}{D}\right)^{n'-1}$$

By substituting into the conventional Prandtl number one obtains

(18) $$\frac{C_p\mu_a}{k} = \frac{C_p\gamma}{k}\left(\frac{V}{D}\right)^{n'-1}$$

and accordingly

(19) $$Re = \frac{D^{n'}V^{2-n'}\rho}{\gamma};\ Pr = \frac{C_p\gamma}{k}\left(\frac{V}{D}\right)^{n'-1};\ St = \frac{h}{C_pG}$$

where

n' = flow behavior index, dimensionless. Between zero and one for pseudo-plastics and is defined by

$$n' = \frac{d\left(\ln \frac{D\Delta P}{4L}\right)}{d\,(\ln 8V/D)}$$

γ = fluid consistency, $lb_m/(ft)(sec)^{2-n'}$.

They also developed a relation between Newtonian and non-Newtonian heat transfer rates which decreased in importance as the flow became fully turbulent.

$$\Delta^{1/3} = \frac{(hD/k)\ \text{non-Newtonian}}{(hD/k)\ \text{Newtonian}}$$

They noted a more gradual transition from laminar to turbulent flow for the highly pseudoplastic fluids.

Finnigan (16), using the same dispersion as in the present work, attempted to correlate the heat transfer data for a mixture of two immiscible liquids. His data was correlated by Equation (7) within about 30% above a Reynolds number of 10,000. At the high flow rates experimental error became large due to the low wall temperatures involved. The heat input was from an electrical coil around the pipe and the heat flux was measured by the electrical input to the coil. This method had the advantage of not requiring a measurable amount of temperature rise in the flowing fluid and the system operated nearly isothermally. The density of the emulsion was computed from the volume fraction of each component. A better correlation was obtained when he used the heat capacity and thermal conductivity of the continuous phase rather than that of the emulsion in calculating the Prandtl number. The viscosity was determined by pressure drop measurements on the same section of vertical pipe used for the heat transfer measurements. An increase in viscosity with increase in flow rate indicated a dilatant fluid and the viscosity was best correlated by the Einstein equation

with an additional correction for higher concentrations and the effect of flow rate.

(21) $$\mu_m = \mu_c\left[1 + 2.5\phi + (3.0 + 1.06w)\phi^2\right]$$

Non-Newtonian Properties

Fluids are classified into two main categories, Newtonian or non-Newtonian, according to their behavior at constant temperature and pressure under imposed shear stresses. The Newtonian fluids are those which show a linear variation between shear stress and the rate of shear; the viscosity is constant in the equation:

(22) $$\tau = \frac{\mu}{g_c}\,(dV/dr)$$

where

τ = the shear stress

dV/dr = the rate of shear.

Non-Newtonian fluids are those in which the viscosity is a function of the rate of shear. There are three classifications of non-Newtonian fluids; (1) Bingham plastics - this type has a constant viscosity but it requires a finite stress before deformation occurs; (2) Pseudoplastic fluids - most non-Newtonian fluids fall into this classification. They are characterized by a decrease in the

the apparent viscosity as the rate of shear increases. The term apparent viscosity is used because the fluid is non-Newtonian. The apparent viscosity is the viscosity of a non-Newtonian fluid at a given rate of shear. This type of definition is necessary because the viscosity often changes with rate of shear; (3) Dilatant Fluids - these are characterized by a rheological behavior opposite to that of pseudoplastics in that the apparent viscosity increases with increasing rate of shear.

The flow behavior index n' is used to characterize the deviation of a fluid from Newtonian behavior as defined on page 13.

Friction Losses - General

The basis for all pressure drop calculations is the general energy equation for steady, isothermal, incompressible flow:

$$\frac{P_2-P_1}{\rho} + \frac{V_2^2-V_1^2}{2\alpha g_c} + g\,\frac{(Z_2-Z_1)}{g_c} = -\overline{W} - \overline{TW}\ .$$

where

P_1, P_2 = the pressure at points 1 and 2, lb_f/ft^2

ρ = the density of the flowing fluid, lb_m/ft^3

V_1, V_2 = the average linear velocity, ft/sec

Z_1, Z_2 = the height above an arbritrary datum, ft

g = acceleration of gravity, ft/sec^2

g_c = conversion factor, $32.2(lb_m)(ft)/(lb_f)(sec^2)$

$\overline{W}$ = work done on fluid between 1 and 2, $(ft)(lb_f)/lb_m$

$\overline{lW}$ = work lost due to friction, $(ft)(lb_f)/lb_m$

α = correction factor for type of flow, $\frac{1}{2}$ for laminar, 1 for turbulent

The other useful equation is the continuity equation:

$$\frac{d(\rho AV)}{dL} = 0 \tag{24}$$

for one-dimensional flow. A is the cross-sectional area of the flow channel. For conduit of uniform cross-section, Equation (23) can be reduced to

$$\frac{\Delta P}{\rho} + \frac{g}{g_c} \Delta Z = -\overline{lW} \quad . \tag{25}$$

Equation (25) is applicable to the steady isothermal flow of an incompressible fluid in a uniform conduit containing no pumps or turbines.

A dimensionless ratio known as the Reynolds number, defined as $Re = DV\rho/\mu$, is used to define the type of flow in the system. Below Reynolds numbers of 2100 the flow is

usually laminar and above 4000 it is usually turbulent with a transition region in between.

A large number of experimental determinations on turbulent flow of fluids have led to the following relationship known as the quadratic resistance law

$$F = \frac{f\rho V^2 A'}{2g_c} \tag{26}$$

F is the resisting force at the wall of the conduit, A' is the surface area of the wall at which F acts, and f is a proportionality factor known as the Fanning friction factor. If this relation is made equal to the lost work term in Equation (25) one obtains

$$\Delta P + \rho \frac{g}{g_c} \Delta Z = - \frac{2\ fL\rho V^2}{D\ g_c} \quad . \tag{27}$$

For a horizontal tube this becomes the familiar Fanning equation:

$$\Delta P_f = - \frac{2fL\rho V^2}{D\ g_c} \tag{28}$$

where ΔP_f = the pressure drop due to friction, lb/ft^2.

Some of the first turbulent flow pressure drop data were obtained by Reynolds (18, p. 120), and his results were reported as the pressure gradient along the tube and not in terms of a friction factor. Blasius compiled all of the available data from other investigators and

presented the following correlation between friction factor and Reynolds number (19, p. 171)

$$f = 0.079\ (Re)^{-\frac{1}{4}} \quad . \tag{29}$$

This equation is accurate for Reynolds numbers from 3000 to 100,000. Stanton and Pannell (40, p. 119) conducted experiments on air, water, and oil for Reynolds numbers up to 500,000 and presented it on a friction factor versus log Reynolds number plot. Nikuradse (19, p. 172) compiled all the available data including his own on water for Reynolds numbers up to 3,240,000 and derived the following semi-empirical equation:

$$\frac{1}{\sqrt{f}} = 4.0 \log (Re \sqrt{f}) - 0.4 \tag{30}$$

which is recommended for determining friction factors in smooth tubes. Other equations were those of Lees (13, p. 56):

$$f = 0.00180 + 0.153\ Re^{-0.35} \tag{31}$$

and Drew (13, p. 56):

$$f = 0.00140 + 0.125\ Re^{-0.32} \quad . \tag{32}$$

Various other equations which consider the roughness of the tubes have been derived but will not be considered here.

Friction Losses for Two Phase Flow

The main problem encountered in predicting friction losses during two-phase flow in pipe lines is the determination of the viscosity of the flowing fluid. There has been considerable theoretical study of the viscosity of suspensions and emulsions. Measurement of the viscosity is often difficult because the fluids are often non-Newtonian and the viscosity is then very dependent upon the method of measurement. Viscosities measured under laminar flow conditions are often different from those measured under turbulent flow conditions. Turbulent viscosities are then obtained by determining the friction loss during the turbulent flow of a two-phase fluid. An apparent viscosity is calculated so that the data fit the usual friction-factor Reynolds number curve for single phase fluids.

The original theoretical work done on the viscosity of suspensions was presented by Einstein (27, p. 396) for the ideal case of spherical particles in an infinite medium. This work was modified by Hatschek (17, p. 163) to account for the viscosity of the dispersed medium. Kunitz (5, p. 127) developed an empirical equation which closely represents the relation between the volume of solute and viscosity of the solution for solutions of sugars, glycogen, casein, and rubber.

(33) $$\mu_m/\mu_c = (1 + 0.5\phi)/(1 - \phi)^4$$

where

μ_m = the viscosity of the medium

μ_c = the viscosity of the continuous phase

ϕ = volume fraction of the dispersed phase

Taylor (41, p. 41) developed an equation for spherical droplets of a dispersed phase and arrived at the relation:

(34) $$\mu_m/\mu_c = 1 + 2.5\phi(\mu_d + 2/5\mu_c)/(\mu_d + \mu_c)$$

where μ_d = viscosity of the dispersed phase.

Becher (3, p. 57) presented several equations which were modifications of Einstein's equation and Taylor's equation;

(35) $$\mu_m/\mu_c = (1 + 2.5\phi + a\phi^2 + b\phi^3 + \ldots)$$

and

(36) $$\ln(\mu_m/\mu_c) = 2.5\left[(\mu_d + 2/5\mu_c)/(\mu_d + \mu_c)\right](\phi + \phi^{5/3} + \phi^{11/3}) .$$

Clayton (9) found that fine emulsions were more viscous

than coarse emulsions at equivalent values of ϕ and the difference increases as ϕ increases. This effect had not been considered by most investigators.

As long as the emulsions were fairly homodisperse the viscosity at high rates of shear varied inversely as the mean globule size (30, p. 367). When the distribution was rather polydisperse the system was less viscous than would be indicated from the mean drop size and the previous relationship. At lower concentrations the variation of viscosity with rate of shear became less marked and the overall viscosity also diminished.

The actual flow of an emulsion must probably involve the slipping or squeezing of small globules through the spaces not occupied by larger ones. The observed variations of viscosity of a concentrated emulsion with concentration and rate of shear could be explained as the work done in distorting the globules and sliding them past each other.

Alves, Boucher, and Pigford (1, p. 388) studied turbulent flow non-Newtonian solutions and suspensions in connection with pipe line design for these fluids. They found the viscosity measured with small pipes and capillary tubes generally agreed fairly well with rotational-viscometer measurements. The non-Newtonian fluids behaved

similarly to Newtonian fluids in the turbulent-flow region, in that they exhibited a relatively constant apparent viscosity. The turbulent viscosity was computed from the turbulent-flow portion of the pipe-line shear diagram. A value of $D\Delta P/4L$ was selected and the linear velocity, V, calculated from the corresponding value of $8W/\rho D^3$. The friction factor was obtained from the Fanning equation

$$f = (D\Delta P/4L)(2g_c/\rho_m V^2). \tag{28}$$

The corresponding Reynolds number was then obtained from the usual friction factor-Reynolds number chart and the turbulent viscosity computed from this Reynolds number.

On data for sludges Caldwell and Babbitt (7, p. 25) found that if the viscosity of the dispersing medium were substituted for the viscosity of the liquid in the Reynolds number, the f vs. Re chart constructed will be almost the same as that for water. This type of result has not been verified by other investigators on different types of slurries. Alves (2, p. 107) reported their data on clay and sewage suspensions. Their systems acted as Bingham plastics and the usual friction factor versus Reynolds number plot was used with viscosity of the continuous phase and density of the slurry. They found the pressure drop to be independent of the yield stress and coefficient

of rigidity. Wilhelm, Wroughton, and Loeffel (2, p. 107) obtained apparent viscosities higher than that for water in cement rock-water suspensions. Binder and Busher (2, p. 107) found the same effect for grain-water suspensions. The following method was recommended to obtain the turbulent viscosity.

(37)
$$f = (\Delta PD/4L)(2g_c/\rho_m V^2)$$
$$Re = DV\rho_m/\mu_m \ .$$

Bonilla, et. al. (5, p. 127) obtained the best viscosity correlation for a chalk water slurry with Hatschek's equation above a Reynolds number of 100,000. An empirical correlation factor was applied to give ± 10% results down to Reynolds number 10,000. The slurry behaved as a Bingham body and it was noted that the effective viscosity of the slurry did not decrease with rise in temperature as rapidly as water. The viscosity data of Orr and DallaValle (28, p. 29) was very inconsistent with any available viscosity equations. Salamone and Newman (32, p. 283) did not consider the variation of viscosity with flow rate for a non-Newtonian suspension.

For sand and water slurries, Smith (37, p. 85) found the pressure drop of the slurry was greater for the slurry than would be obtained with a liquid of density equal to that of the slurry. This became less apparent at higher

velocities. An equation was derived but required that the diameter of the particles be known and that they be closely sized.

Spells (39, p. 79) correlated the data of several investigators on slurries of sand in water and boiler ash in water. For a certain velocity range immediately above the minimum velocity, where separation of phases begins, the friction losses were considerably greater than that of the equivalent true fluid; this being a fluid of density equal to that of the slurry and viscosity equal to that of water. As the rate of flow increased the pressure gradient approached the equivalent true fluid value and eventually became identical with it. He defines a standard velocity at which the pressure gradients for the slurry and its equivalent true fluid became identical. Thus, at the standard velocity the friction factor is the same for the slurry as for the equivalent true fluid. The values for the minimum velocity (V_m) and the standard velocity (V_s) were developed by semi-empirical means.

The variables are particle diameter, d, density of the continuous phase, ρ_c, density of the dispersed phase, ρ_d, and the acceleration due to gravity, g. The apparent weight of an immersed particle is proportional to $(\rho_d - \rho_c)$ where ρ_d and ρ_c are the densities of the dispersed and continuous phases respectively. These variables

can be arranged into the dimensionless groups of V^2/gd and $\rho_c/(\rho_d - \rho_c)$. Since the flow in a pipe is concerned, a relationship with Reynolds number is assumed. Thus the following equation is developed.

$$\frac{V^2}{gd}\,\frac{\rho_c}{(\rho_d - \rho_c)} = \psi\left(\frac{DV\rho_m}{\mu}\right) \tag{38}$$

The minimum velocities were obtained by noticing when the particles in suspension began to settle out and the standard velocities were the values at which the friction factor became the same for the slurry as for the equivalent true fluid.

From the available data Spells formulated the following equations.

$$V_m^{1.225} = 0.0251\ gd\ \frac{D\rho_m}{\mu}^{0.775}\ \frac{\rho_d - \rho_c}{\rho_c} \tag{39}$$

and

$$V_c^{1.225} = 0.0741\ gd\ \frac{D\rho_m}{\mu}^{0.775}\ \frac{\rho_d - \rho_c}{\rho_c}$$

Winding (44, p. 527) investigated the flow properties of pseudoplastic fluids. For experimental data on GR-S latices (synthetic rubber) for flow in the turbulent region, the use of the Fanning equation was recommended and the graph of friction factor against Reynolds number was used with the limiting viscosity at infinite shear in the computation of the Reynolds number.

Finnigan (16, p. 92) found a linear increase in the viscosity with increase in flow rate for a petroleum solvent and water emulsion. This type of variation would indicate a slightly dilatant type of fluid. The viscosity was calculated from pressure drop data on a vertical test section. The Fanning friction factor was computed from the pressure drop data and the Reynolds number determined from Nikuradse's equation for smooth tubes;

$$1/\sqrt{f} = 4.0 \log (Re \sqrt{f}) - 0.40 . \tag{30}$$

The apparent viscosity was determined from the Reynolds number.

CHAPTER 3

EXPERIMENTAL EQUIPMENT

The apparatus used was designed to carry out simultaneous investigations of the heat transfer characteristics and the viscosity of fluids. The general piping layout was similar to that used by Finnigan (16, p. 28) in his recent work on the same emulsion. Figure 1 presents a schematic diagram of the important features of the equipment used. The work of the author did not include laminar flow viscosities or light transmittancy measurements which were made simultaneously by Cengel (8) and this portion of the equipment will be mentioned only briefly.

The fluid was drawn out of a supply tank by a pump and to the horizontal test section where the heat transfer and pressure drop measurements were made. An orifice meter was installed between the pump and the test section. A baffled mixing tank and a heat exchanger were on the downstream side of the test section and from the heat exchanger the fluid was carried back to the supply tank. The supply tank, agitator, and pump were the same as those used by Finnigan (16) and are described in detail by him.

FIGURE 1

SCHEMATIC FLOW DIAGRAM

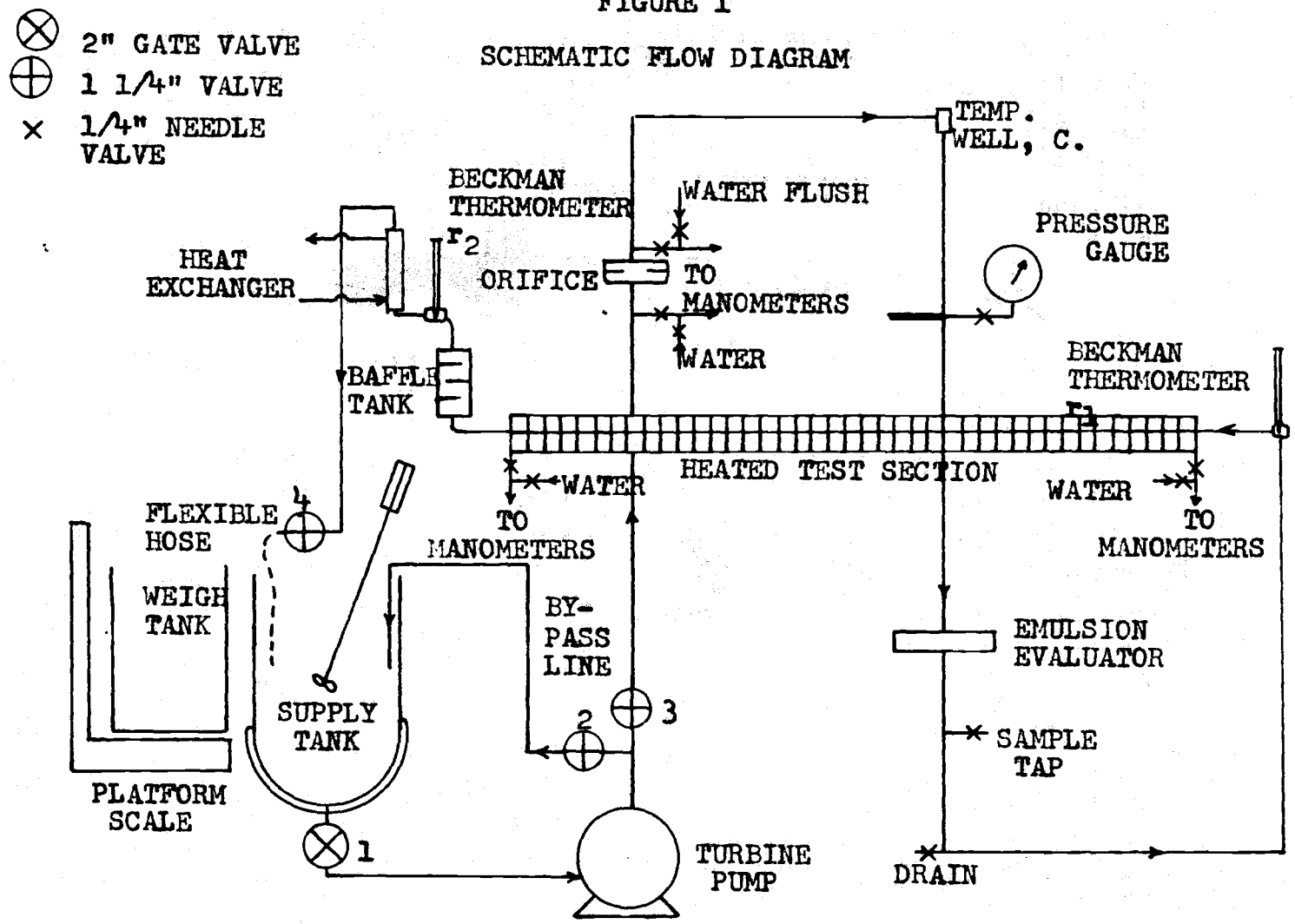

Supply Tank and Pump

A stainless steel supply tank was used to charge and mix the liquids. The instability of the emulsions made it necessary to install a propellor-type agitator on the edge of the tank. A bypass line on the discharge side of the pump allowed the flow rate of fluid through the test section to be varied without increasing the pressure in the system. The bypass line also contributed greatly to the circulation and mixing of the fluid in the tank. Figure 2 is a photograph of the test equipment.

The pump was a Fairbanks-Morse bronze turbine pump driven by a three horse power electric motor.

In the piping system used the maximum achievable water flow rate obtainable was about 24 gallons per minute.

Main Piping System

The entire piping system was constructed of copper and brass piping with the exception of a stainless steel supply tank, a flexible length of rubber hose and a short sight glass. The piping between the supply tank and the pump inlet was nominal 2-inch red brass pipe. A 2-inch gate valve (No. 1) was installed in this line to allow for separate draining of the system. Downstream from the pump the piping was 1¼-inch brass pipe with a short piece of synthetic rubber hose on the exit of the pump to dampen

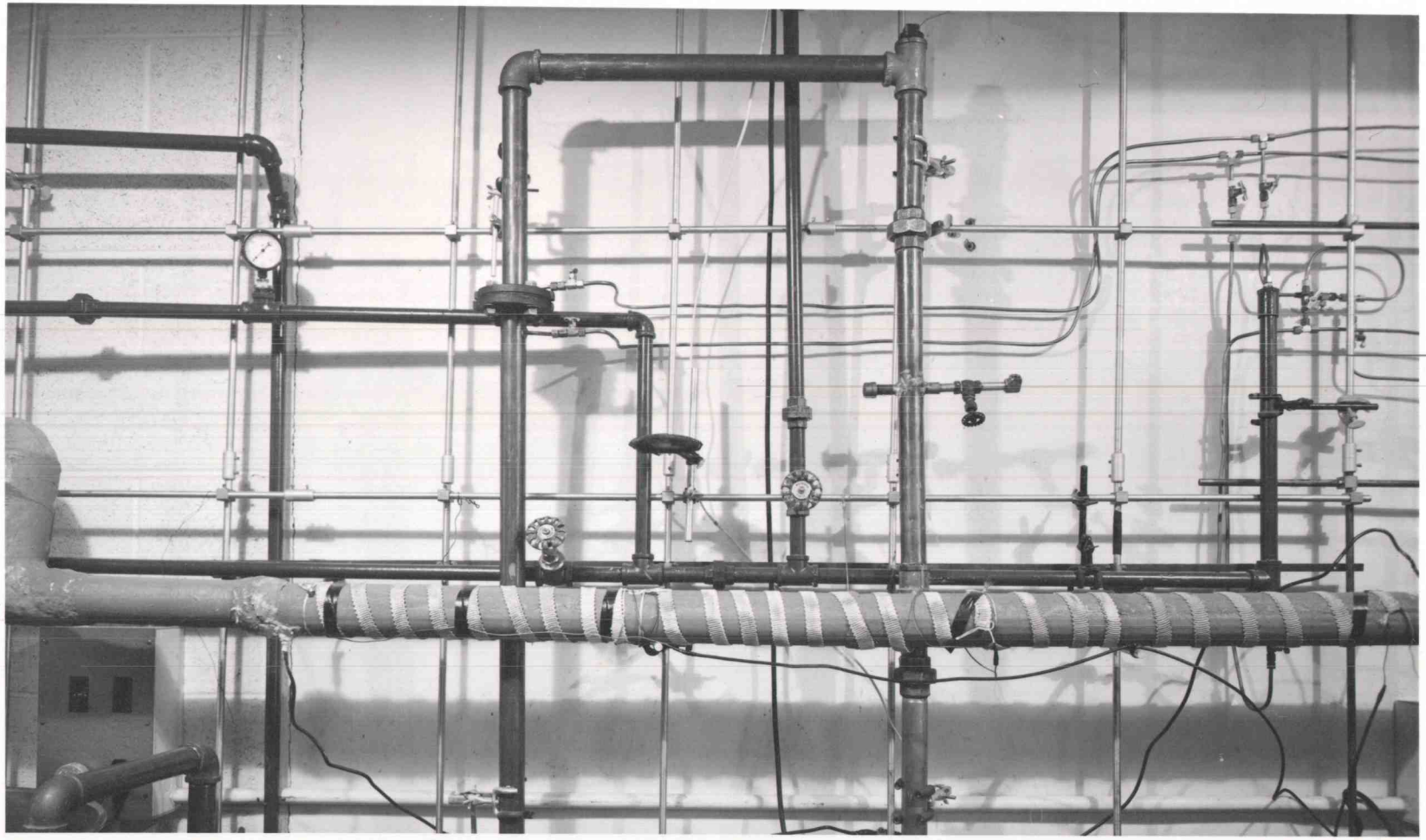

FIGURE 2
PHOTOGRAPH OF EQUIPMENT

vibrations. All threaded pipe connections were sealed with "Cyl-Seal" high pressure sealant manufactured by the West Chester Chemical Company. This was effective in preventing leakage and was inert to the solvent.

Eight brass unions were placed strategically for ease of assembly and disassembly of the system. A plug was inserted below the emulsion evaluator for ease in draining as show in Figure 1.

The measurements of the mass flow rate were made by timing the flow of a predetermined weight of fluid by a stopclock.

Orifice Meter

The brass orifice meter used in all of the experimental runs was made and accurately calibrated by Finnigan (16, p. 96) in previous work. It was necessary to make spot calibration checks on the meter. The calibration curve of the orifice is given in Appendix B.

The average pipe diameter was 1.366 $\pm$ 0.002 inches and the orifice opening was 0.695 inches. The plate was made of 1/16-inch brass and the edge of the orifice was 1/64-inch thick. The orifice taps were 0.237 feet apart. Other details of the construction and calibration of the orifice meter are given in the thesis by Finnigan (16, p. 35).

Test Section

The test section was a horizontal 10-foot length of smooth-wall copper condenser tubing, 7/8-inch O.D., 16 BWG wall, and 0.745 ± 0.003 inches I.D.

Two brass nipples were brazed onto the tubing 6 feet (or 97 diameters) apart and 1/32-inch holes bored through the tubing. Any burrs were removed by passing an emery cloth through the test section. This defined the length of the test section for pressure drop measurements. A calming section of 3 feet (or 48 diameters) preceded the test section and a length of one foot (or 16 diameters) followed the second pressure tap.

The heating was accomplished by a Nichrome ribbon having an effective length of 17.1 feet. The ribbon was 1-inch wide, 0.005 inches thick, and had an overall resistance of about 1.77 ohms. Nine thermocouples were used to measure the tube-wall temperature, three near each pressure tap and the remaining three equally spaced between. The relative locations and the numbering arrangement of the thermocouple junctions are shown in Figure 3. The thermocouples were made of number 30 B and S gauge copper and constantan wires supplied by the Leeds and Northrup Company. The thermocouples were positioned into grooves which had been previously tinned with solder. The ends of the leads were enameled with General Cement Insulating and

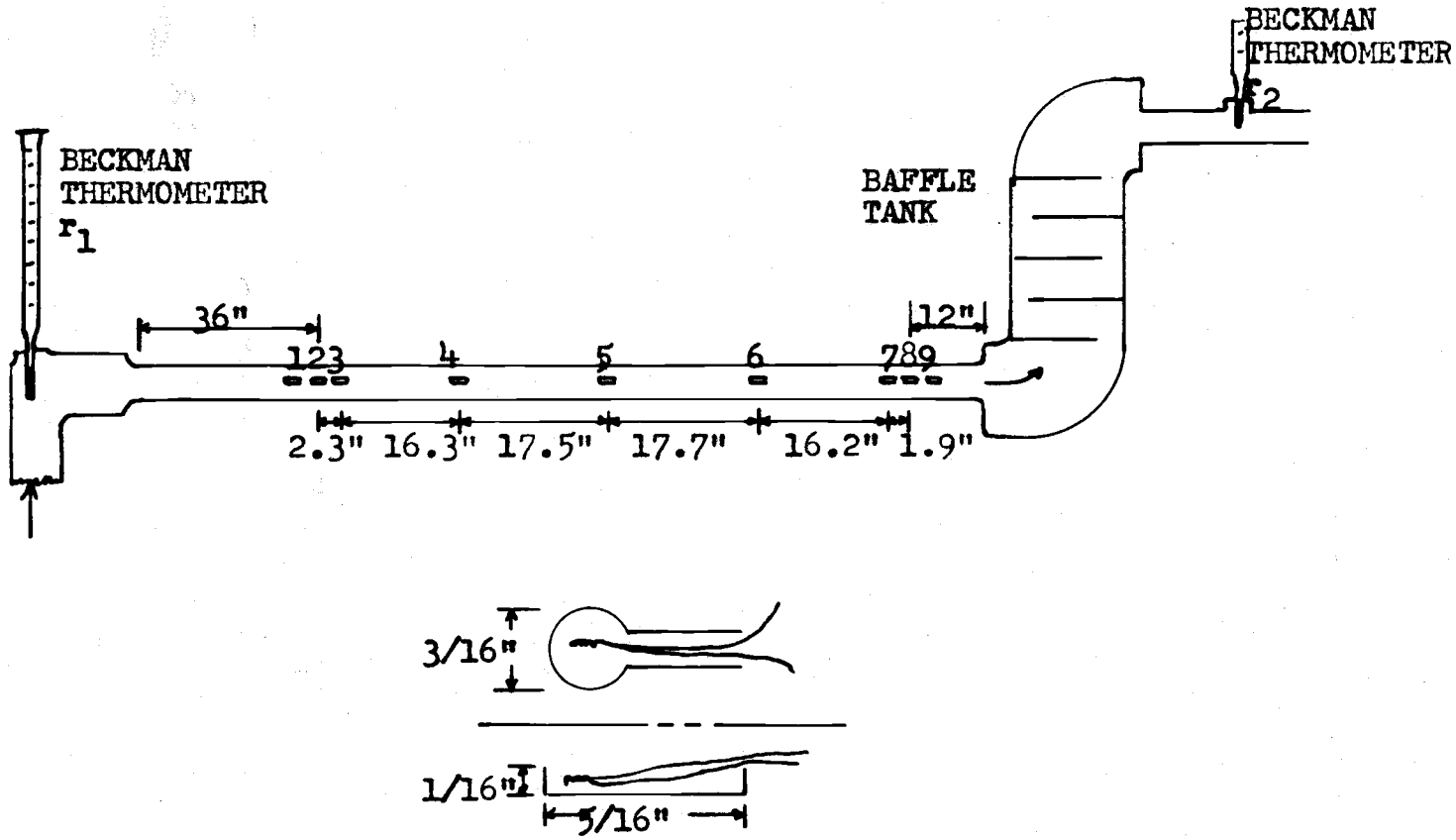

FIGURE 3

A DIAGRAM OF THE RELATIVE LOCATIONS OF THE THERMOCOUPLES

AND A DETAILED SKETCH OF A THERMOCOUPLE GROOVE

Dipping Varnish. About 1/8-inch was scraped clean on the ends and the wires were twisted tightly together. The junction was then warmed and thrust into a pool of solder in the groove. The area around the junction was painted with the insulating varnish and a piece of "Saran" wrap was placed under the lead wires near the junction, another layer of varnish was applied and a large piece of Saran wrap covered the pipe for a length of about 4-inches. A layer of asbestos paper was placed over the whole section to be heated. The Nichrome heating ribbon was wound over this and a multilayer corrugated insulation was used to cover the section to reduce heat losses. A cutaway model of the test section is shown in Figure 5.

The nine thermocouple leads and another thermocouple in the flow system (designated as thermocouple c) were connected to a 2-pole 12-position non-shorting steatite rotary switch as shown in Figure 4. The cold junction leads were brought from the selector switch to a thin glass tube filled with oil and immersed in a thermos bottle filled with crushed ice in equilibrium with water. The thermocouple voltages were measured with a Leeds and Northrup potentiometer and a very sensitive Leeds and Northrup No. 2430 galvanometer. The thermocouples were then calibrated within about 0.2°F with a standard thermometer.

The heater coil was connected to a "Variac" and then

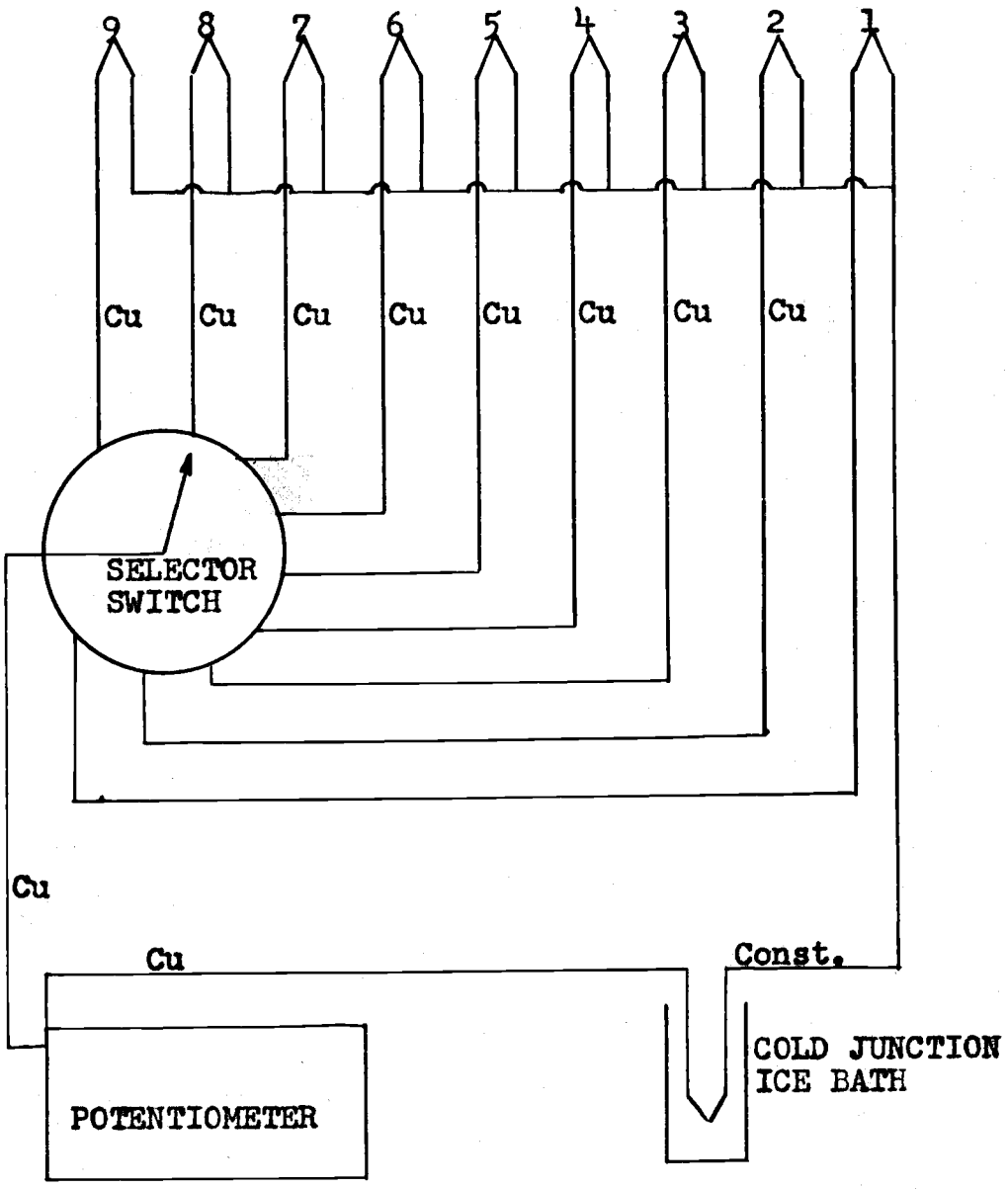

NOTE: ONLY ONE GANG OF THE TWO-GANG SWITCH IS SHOWN

FIGURE 4

THERMOCOUPLE WIRING DIAGRAM

to a constant voltage transformer which reduced the line voltage of 220 volts to 110 volts. This made it possible to supply about 3200 watts to the heating coil without overloading the equipment. An A. C. voltmeter and an ammeter were used to measure the total power input to the test section. Figure 6 shows the test section power supply.

Manometer System

The pressure differences across the orifice meter and the test section were measured with U-tube differential manometers. Two manometers were provided for each pressure drop measuring section. One of these manometers contained mercury and the other contained carbon tetrachloride. The carbon tetrachloride contained a small amount of iodine to give a sharp meniscus for ease in reading. The pressure transmitting medium in all cases was water and a flushing system was arranged so that if any of the emulsion from the piping system moved into the pressure transmitting lines it could be easily flushed out.,

The manometers were made of heavy-wall "Pyrex" glass tubing and were about 3-feet in length. The manometers were connected to the brass seal pots by short lengths of rubber tubing and were securely wired down to prevent any leaks. Meter sticks were fastened to the panel to serve

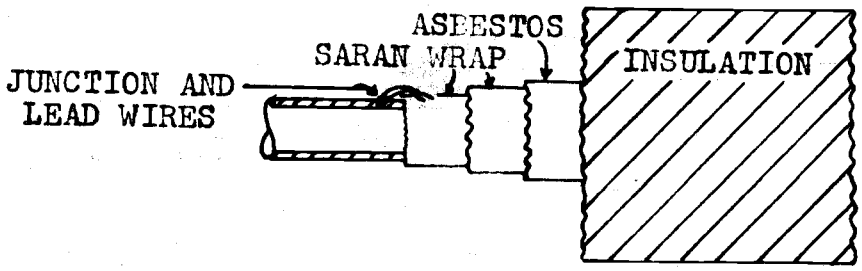

FIGURE 5

CUTAWAY OF TEST SECTION

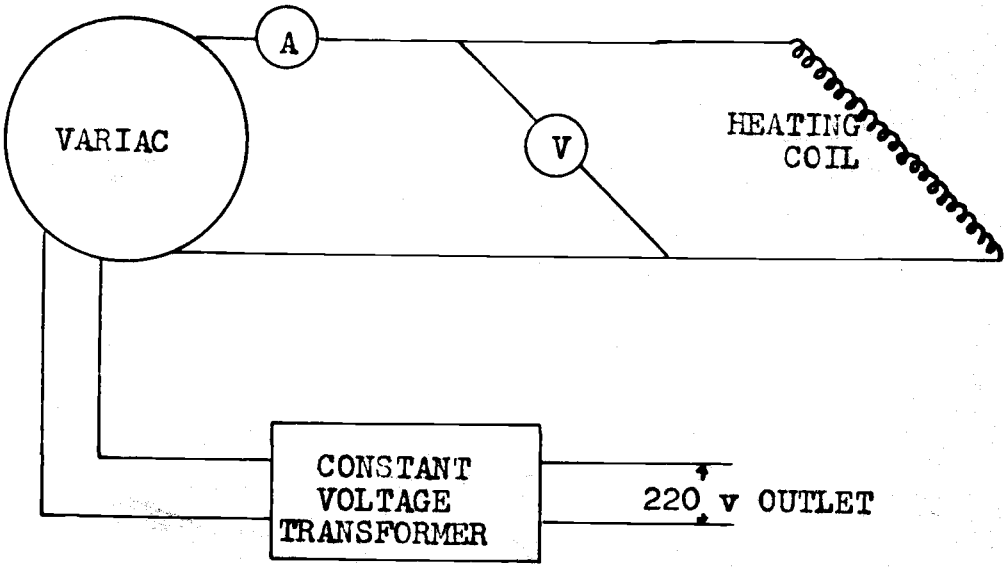

FIGURE 6

POWER SUPPLY SYSTEM TO HEATING COIL

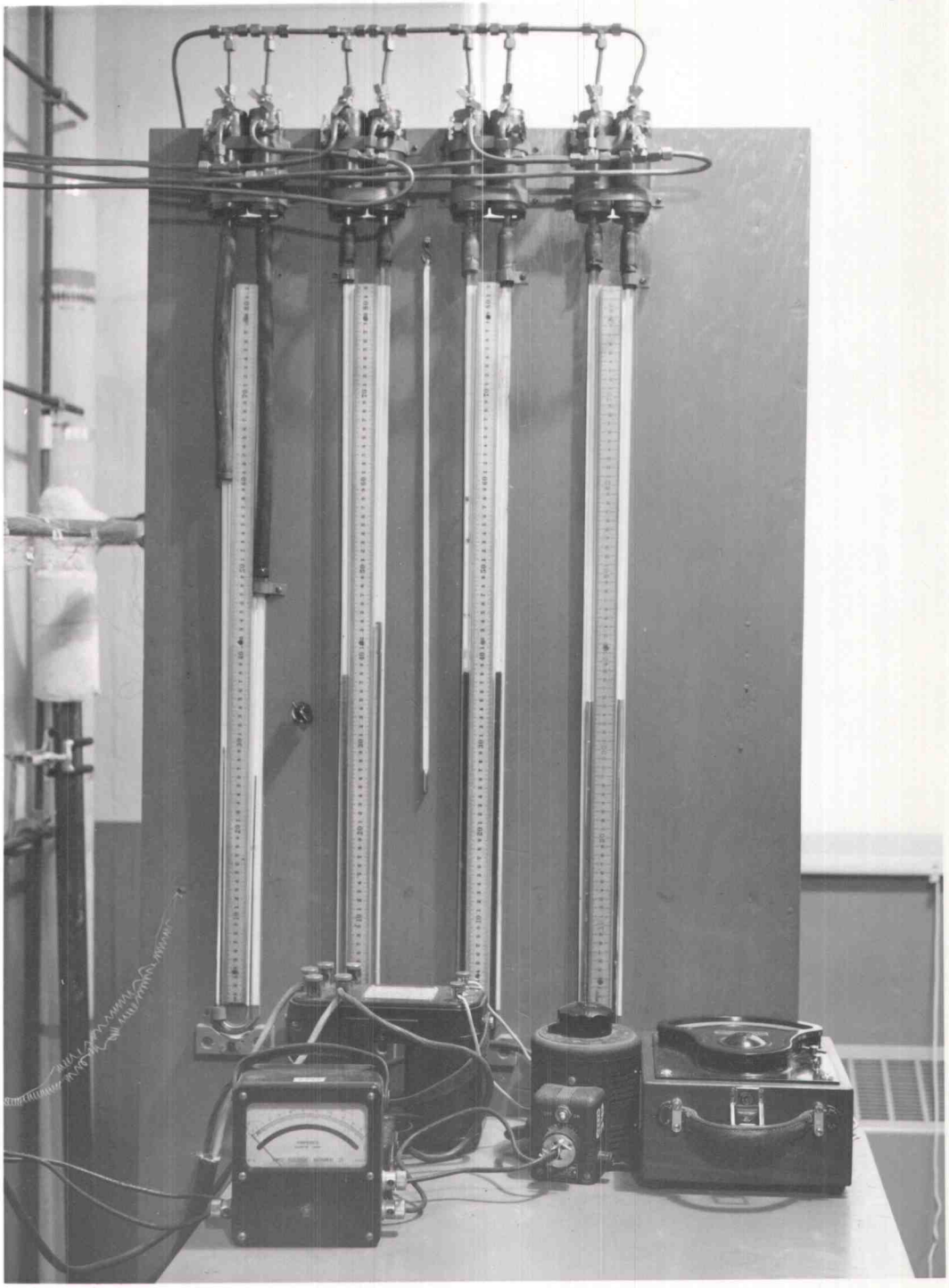

FIGURE 7

MANOMETER BOARD ARRANGEMENT

as length scales for the manometers as shown in Figure 7.

The pressure transmission lines were made of 1/4-inch copper tubing. These lines were run horizontally for at least three feet to prevent transfer of the less dense two-phase fluid to the vertical portions of the lines. A series of ¼-inch brass needle valves allowed the flushing water to be admitted to the lines either individually or in pairs.

Thermometers

A pair of Beckman thermometers with 0.01°C scale divisions were used to measure the change in bulk temperature of the fluid as it passed through the heated test section. The Beckman thermometers were calibrated in a constant temperature bath using a standard thermometer with ± 0.02°C. The Beckman thermometer designated as r_1 was used to measure the temperature of the fluid entering the test section.

The thermometer wells were made by drilling a 1/2-inch hole in a 1¼-inch pipe plug and brazing on a 2 3/8-inch piece of 3/4-inch copper tubing. A thin sheet of copper was brazed to the bottom of the well. The thermometer wells were filled with light oil and placed in the positions shown in Figure 3 to measure the bulk temperature. Magnesia insulation was packed around the pipe near the thermometers to prevent effects due to ambient

temperature.

Although the tests were run only under turbulent flow conditions, a baffle tank was built into the piping between the end of the test section and the second Beckman thermometer (r_2) as shown in Figure 3. The baffle tank was constructed from an 8-inch piece of 2-inch copper pipe. Two-inch brass elbows were brazed onto the ends after the five thin copper baffles had been installed. The baffles were circular with one side cut away and placed such that the fluid was continuously changing direction.

Down-stream from the second Beckman a heat exchanger was installed to cool the fluid to the bulk temperature of the fluid in the tank. The exchanger was a small Ross "BCF" exchanger and the fluid flowed through the tubes with cooling water flowing co-currently in the jacket. The water rate through the heat exchanger was used to control the system at the desired temperature and maintain it at steady-state.

The description of the capillary tubes, used to measure the laminar flow viscosity, and the Emulsion Evaluator, which was used to compare the light transmitted by the various emulsions, can be found in the thesis by Cengel (8).

CHAPTER 4

EXPERIMENTAL PROCEDURE

Scope of the Investigation

The investigation was made to determine the pressure drop and heat transfer characteristics of a dispersion of two immiscible liquids flowing in a circular tube. The investigation was confined to the turbulent region because of the problems encountered when the phases begin to separate during laminar flow.

The liquids used were water and a petroleum solvent known as "Shellsolv 360" manufactured by the Shell Oil Company. These two liquids are insoluble in each other and no tendency toward stable emulsion formation was noted during the tests. The compositions to be used during the tests were charged to the tank before each series of runs and during the runs samples were taken in 500 ml. graduated cylinders to determine the actual composition of the mixture. The samples were sealed tightly and allowed to stand overnight and then the volume of each component after separation was measured to calculate the actual compositions. All samples were taken at a location upstream from the test section.

The physical properties of water were taken from the literature and the properties of the petroleum solvent,

which had not been supplied by the manufacturer, were measured by Wang and Knudsen (43, p. 1667) and Finnigan (16, p. 129). The individual properties of the liquids are presented in Appendix B.

The mixtures were prepared by charging a weighed amount of water to the supply tank and allowing this to circulate for several minutes through the entire piping system. The required amount of solvent was then added to the supply tank and the creamy white color of the emulsion became immediately apparent. The emulsion was considered well mixed when the light transmittancy became constant, no layer of solvent was evidenced in the tank, and consecutive pressure drop readings became constant. This required from about one to five hours depending on the composition. The compositions investigated were:

1. Pure water
2. 5% solvent in water
3. 20% solvent in water
4. 35% solvent in water
5. 50% solvent in water
6. Pure solvent

In the composition range between about 65% solvent in water and 15% water in solvent, Finnigan (16) found it very difficult or impossible to maintain a uniform and sufficiently stable composition. No measurements were

attempted in this range.

At the end of a series of runs the liquids were allowed to separate in the supply tank and the clear solvent decanted off and reused. The water and a layer of dirt which collected at the interface were flushed out. A small amount of contamination seemed to be present at the interface after every series of runs but their removal each time prevented a build-up which might affect the properties of the emulsion.

Pressure Drop and Orifice Measurements

After each series of runs the manometer lines were flushed with water and closed until the next series of runs had begun. When beginning a run the globe valve on the return line was closed but a positive gauge pressure of about 5 psig was maintained in the system by adjusting the bypass valve. The needle valves were opened on the manometer lines and the manometers were allowed to come to zero. The manometers on the orifice meter did not balance at the zero point except when pure water was being used and a small computation was required to compute the actual zero point. Since the test section was horizontal, no effect was caused by the various fluids present in the test section. The return line was then opened, closed, and a check made to see if the manometers returned to their

zero positions. The manometer lines were flushed and this procedure repeated until consistently satisfactory readings were made.

The valve at the end of the discharge line was opened partially and by adjusting the bypass valve and the return line valve the desired rate of flow and pressure in the system could be obtained. For the low flow rates the carbon tetrachloride manometers were used and these were closed off and mercury manometers for the high range were used. In the intermediate range of flow both manometers were used. The manometer readings ranged from about 1 centimeter of carbon tetrachloride to about 40 centimeters of mercury.

Any fluctuations which were present in the manometer columns were usually dampened by throttling down the needle valves on the manometer board. The air temperature was always taken to be used in calculating the effective densities of the manometer fluids.

Heat Transfer Measurements

The power input to the heating ribbon was usually adjusted by the "Variac" so that about 5°F difference was obtained between thermocouples No. 1 and No. 3. This is the approximate driving force. The cooling water to the heat exchanger was then adjusted to remove the heat and

return the fluid to the tank at the temperature of the tank. The system was considered at thermal equilibrium when the temperature at Beckman r_1 changed by no more than 0.04°F in 10 minutes and the wall temperatures showed no measurable change. The total power input was measured by a voltmeter and ammeter in the power supply system. All of these readings were converted into power units and compared with the power as measured by the temperature rise in the fluid passing through the test section.

Since the application of the general energy equation requires isothermal conditions, the properties of the fluid were evaluated at an average bulk temperature. This assumption was considered accurate enough for the calculations involved.

Flow Rate Measurements

The mass flow rate was calculated from the determinations of Finnigan (16, p. 95) on the orifice coefficient and his graph of flow rate in lb/sec versus

$$\rho_m\left[\Delta P + L' \frac{g}{g_c}(\rho_m - \rho_c)\right] .$$

where

ρ_m = density of the emulsion, lb/ft^3

ΔP = the pressure drop across the orifice, lb/ft^2

L' = height correction for the orifice taps, ft

ρ_c = density of the continuous phase, lb/ft^3.

At each concentration several checks were made by using a stopwatch to time the discharge of predetermined weight of the solution into a weighing tank. These values checked within about 5% of the values given by Finnigan's curve.

Summary of Experimental Procedure

At each flow rate of each series of runs the following data collecting procedure was used:

(a) Manometers zeroed and flushed if necessary.

(b) Establish an approximately determined flow rate through the system by adjusting the bypass valve and return line valve.

(c) Adjust the Variac to give the approximate temperature rise desired.

(d) Stabilize the Beckman temperature readings; read and record them.

(e) Read and record all thermocouple readings of test section wall temperatures and air temperature.

(f) Read and record the orifice and test section manometer readings.

(g) Read and record the power input and the system pressure.

(h) At least twice during a series of runs - check the flow rate and take a composition sample.

The above procedure was repeated for each flow rate during a series of runs. Steady-state was usually reached from 20 minutes to two hours after changing the flow rate.

CHAPTER 5

CALCULATION PROCEDURE

Flow Rate

The equation used to determine the flow rate was

$$(40) \qquad w = C_D A_0 \left[\frac{2 g_c \rho_m \left[-\Delta P - \frac{g}{g_c} (\rho_m - \rho_c) L' \right]}{1 - \left(\frac{D_0}{D_1} \right)^4} \right]^{\frac{1}{2}} .$$

where

C_D = the orifice coefficient, dimensionless

L' = the distance between orifice taps, ft

A_0 = cross-sectional area of orifice opening, ft^2

D_0 = diameter of the orifice, ft

D_1 = diameter of the pipe, ft

All of the constants were determined by Finnigan (16, p. 98) and verified by the author with a final result of

$$(41) \qquad w^2 = K \rho_m \left[-\Delta P - \frac{g}{g_c} L' (\rho_m - \rho_c) \right]$$

The data was plotted as log w versus log $\rho_m \left[-\Delta P - \frac{g}{g_c} L' (\rho_m - \rho_c) \right]$ and gave a straight line.

A sample calculation could be illustrated by using

the data of run No. 1, 35% solvent in water (35-1) for a 34.2% emulsion of solvent in water at 71°F.

$$\rho_m = \rho_w \text{ @ } 71^\circ F \left[(S.G._w)(vol.fr.w) + (S.G._s)(vol.fr.s) \right]$$

$$\rho_m = 62.31 \left[(1.0)(0.658) + (0.784)(0.342) \right] = 57.70 \text{ lb}_m/\text{ft}^3$$

$$\frac{g}{g_c} L' (\rho_m - \rho_c) = \frac{32.2}{32.2} (0.237)(62.31 - 57.70)$$

$$= 1.09 \text{ lb}_f/\text{ft}^2$$

$$\Delta P = \frac{(13.54 - 0.999)(62.43) \text{ lb}_m/\text{ft}^3}{(304.8 \text{ mm/ft})} \quad (\text{mm Hg})$$

$$= (2.568)(45) = 115.6 \text{ lb}_f/\text{ft}^2$$

$$\rho_m \left[(\Delta P + \frac{g}{g_c} L' (\rho_m - \rho_c) \right] = 57.59 \ (115.6 + 1.12) = 6720 \text{ lb}^2/\text{ft}^5$$

From Figure 20 w = 1.08 lb_m/sec

<u>Fanning Friction Factor</u>

The general energy equation presented in Chapter 2 was reduced to:

(28) $$\Delta P = \Delta P_f$$

for the horizontal test section which was used for pressure drop measurements. The pressures at P_1 and P_2 as

shown in Figure 8 must be calculated and the difference taken to obtain the pressure change between points 1 and 2. By summing the pressures in each leg and taking the difference, the following equation results:

$$-\Delta P = b\,(\rho_b - \rho_c)$$

where

$$(\rho_b - \rho_c) = \rho_e \; .$$

The effective density of mercury and carbon tetrachloride under water is given in Figure 16 in Appendix B. The Fanning friction factor is given by the relationship,

(43) $$f = \frac{g_c D}{2\rho V^2}\left(-\frac{dP_f}{dL}\right)$$

which can be altered to give

(43-a) $$f = \frac{\pi^2}{32}\,\frac{g_c D^5}{L}\,\frac{\rho_m \Delta P}{w^2} \; .$$

since

$$g_c = 32.2 \text{ lb}_m\text{ft/lb}_f\text{sec}^2$$

$$D = 0.062 \text{ ft}$$

$$L = 6.0 \text{ ft}$$

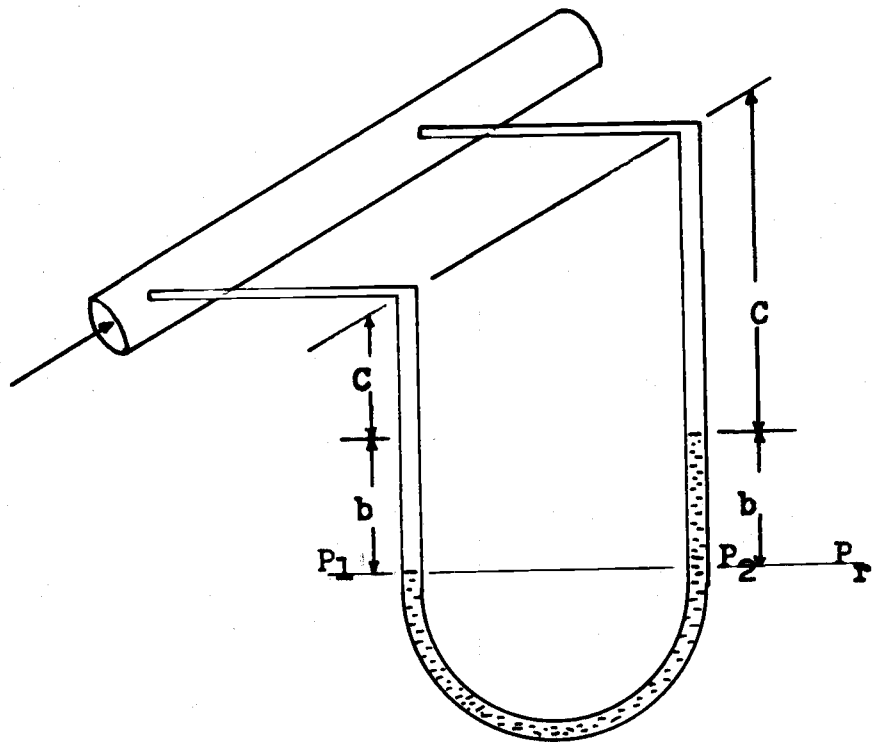

FIGURE 8

MANOMETER CONNECTED ACROSS A HORIZONTAL TUBE

$$f = \frac{\pi^2(32.2)(0.062)^5}{(32)\quad(6.0)}\left(\frac{\rho_m \Delta P}{w^2}\right)$$

(43-b) $$f = 1.516 \times 10^{-6}\left(\frac{\rho_m \Delta P}{w^2}\right)$$

A sample calculation for Fanning friction factor on run 35-1 is given below.

$$f = 1.516 \times 10^{-6}\ (57.70)\frac{(38)(2.568)}{(1.08)^2}$$

$$f = 0.007319$$

where

$\rho_m = 57.70$ lb/ft^3

$b = 38$ mm Hg

$\theta = 2.568$ lb/ft^2/mm Hg

$w = 1.08$ lb/sec

<u>Reynolds Number and Viscosity</u>

The Reynolds number was given by:

(44) $$Re = \frac{DV\rho}{\mu}$$

and can be altered by using:

(45) $$V = \frac{w}{\rho}\ \frac{4}{\pi D^2}$$

giving:

(44-a) $$Re = (4w/\pi D\mu)$$

and

(44-b) $$Re = \frac{(4)(1488)}{(\pi)(0.062)} \frac{w}{\mu} = 30{,}600 \frac{w}{\mu} .$$

where

$D = 0.062$ ft

$\sigma = 1488$ centipoise/(lb_m)(ft)(sec)

μ = viscosity, centipoise

The viscosity was calculated from the relation between friction factor and Reynolds number as given by Nikuradse.

(30) $$\frac{1}{\sqrt{f}} = 4.0 \log (Re \sqrt{f}) - 0.40$$

By substituting the equation for the Reynolds number from Equation (44-b), this equation can be altered to give

(30-a) $$\frac{1}{\sqrt{f}} = 4.0 \log w\sqrt{f} - 4.0 \log\mu + 4.0 \log 30{,}600 - 0.40 .$$

The graph of $1/\sqrt{f}$ versus $\log w\sqrt{f}$ (Figure 10) gives various parameters for the different emulsions. On this graph a straight line parallel to the line drawn for pure water would indicate a constant viscosity. The only series of data showing this tendency were the pure solvent and pure

water. As the compositions increased the lines became more curved and had a slope increasingly different from that of pure solvent and pure water. From Figure 10 arbitrarily chosen values of friction factor were used to determine flow rate. The values of flow rate were substituted into Equation (30-a) to calculate viscosities for making Figure 11. From this figure the viscosity could be determined for any given flow rate at a given composition.

A sample calculation of Reynolds number on run 35-1 is given below.

$$w = 1.08 \text{ lb/sec}$$

From Figure 11

$$\mu = 3.19 \text{ centipoise}$$

$$Re = \frac{(30,600)(1.08)}{(3.19)}$$

$$= 10,360$$

Temperatures and Temperature Rise

The wall temperatures in the test section were measured by thermocouples and the bulk temperature of the fluid was measured by Beckman thermometers as shown in Figures 2 and 4.

The temperature driving force was computed by using the integrated average of thermocouples No. 3, 5, and 6. These thermocouples had been properly embedded and gave

consistent readings. Thermocouples No. 4 and 7 gave temperature readings which were high. This error was probably due to the junction contact being made outside of the groove. The thermocouple calibration curve is given in Appendix B. The bulk temperature was calculated from the average of the two Beckman thermometer readings.

The average wall temperature was given by the equation

$$t_w = \frac{(t_3+t_5)\ l_1 + (t_5+t_6)\ l_2}{2\ (l_1 + l_2)} \quad . \tag{46}$$

where

t_3, t_5, t_6 = temperatures measured by thermocouples No. 3, 5, and 6, °F

l_1, l_2 = lengths between thermocouples No. 3 and 5 and 5 and 6, in.

l_1 = 33.8 in.

l_2 = 17.7 in.

$$t_w = \frac{33.8\ (t_3+t_5) + 17.7\ (t_5+t_6)}{103.0} \tag{46-a}$$

An example of this calculation for the previously used example is:

$$t_w = \frac{(33.8)(76.14+77.76) + 17.7\ (77.76+77.76)}{103.0}$$

$$t_w = 77.23^oF$$

$$t_b = t_{r_1} + 0.38\ (t_{r_2} - t_{r_1})$$

$$t_b = 0.62\ t_{r_1} + 0.38\ t_{r_2}$$

(The value of 0.38 was used to give the bulk temperature at the position of the average wall temperature.)

$$t_b = (0.62)(71.06)+(0.38)(72.29)$$

$$t_b = 71.53^oF$$

$$t_w - t_b = 77.23 - 71.53$$

$$= 5.70^oF$$

$$t_{r_2} - t_{r_1} = 72.29 - 71.06$$

$$= 1.23^oF$$

The temperature profile for run 35-1 is given in Figure 9.

Stanton Number and Prandtl Number

The general heat balance equation might be given as

$$h_m(\pi DL)(t_w - t_b) = \frac{D^2\pi}{4}\ GC_p\ (t_{b_2} - t_{b_1}) \quad . \tag{47}$$

The definition of the Stanton number is

$$St = (h_m/GC_p) \quad .$$

and the relation for evaluating the Stanton number is rearranged to give

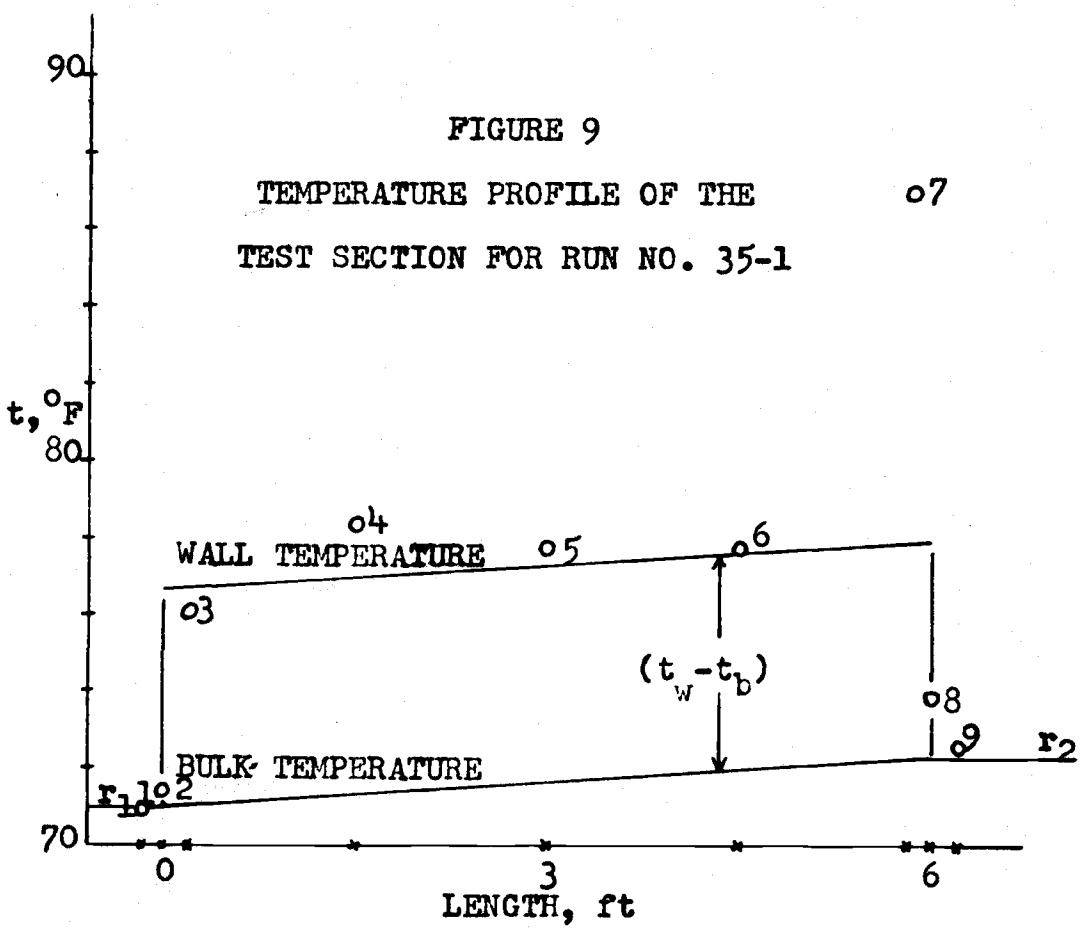

FIGURE 9

TEMPERATURE PROFILE OF THE TEST SECTION FOR RUN NO. 35-1

$$St = \frac{D}{4L} \frac{t_{b_2} - t_{b_1}}{(t_w - t_b)_{l.m.}} .$$

where the terms are defined as:

t_w = temperature of the pipe wall, °F

t_b = the bulk temperature, °F

t_{b_1}, t_{b_2} = the bulk temperature at the beginning and end of the heat section, °F

G = mass velocity, $lb_m/(ft^2)(sec)$

C_p = heat capacity, Btu/(lb)(°F)

h_m = the mean heat transfer coefficient, $Btu/(ft^2)(hr)(°F)$

Since

$D = 0.062$ ft

$L = 6.0$ ft

then

(48-a) $$St = 2.58 \times 10^{-3} \frac{(t_{b_2} - t_{b_1})}{(t_w - t_b)_{l.m.}}$$

The Prandtl number is defined as

$$Pr = (C_p \mu / k) .$$

where

Pr = the Prandtl number, dimensionless

k = the thermal conductivity, Btu/(lb)(°F)(ft^2)/ft

$$C_{p_m} = (C_{p_w})(wt.fr.w) + (C_{p_s})(wt.fr.s)$$

is calculated from Figure 11 knowing the flow rate.

$k = k_c$ = the thermal conductivity of the continuous phase.

A sample calculation involved the Stanton number and Prandtl number for the previously used example is:

The average wall temperature, $t_w = 77.23$ °F

The average bulk temperature, $t_b = 71.53$ °F

The temperature rise of the fluid = 1.233 °F

Viscosity, $\mu = 3.19$ centipoise

Thermal conductivity at 71.5 °F = 0.346 Btu/(lb)(°F)(ft)

$$C_p = 0.711 + (0.289)(0.4676)$$

$$C_p = 0.846 \text{ Btu/(lb)(°F)}$$

$$St = \frac{(2.58 \times 10^{-3})(1.233°F)}{(77.23 - 71.53)°F}$$

$$St = 0.558 \times 10^{-3}$$

$$Pr = \frac{(0.846)(3.19)(2.42)}{0.346}$$

$$= 18.88$$

$$St(Pr)^{2/3} = (0.558 \times 10^{-3})(18.88)^{2/3}$$

$$= 0.00396$$

Heat Transfer Coefficient

The heat transfer coefficient is the individual coefficient between the surface of the pipe and the fluid. Although the temperatures measured were the temperature of the outside wall of the pipe, the resistance of the pipe wall is negligible and the temperature of the outside and inside of the pipe are the same within the accuracy of the measuring instruments. The defining equation for heat transfer coefficient is given in Equation (47). A more workable form can be made by incorporating some of the terms into the Stanton number which gives:

$$h_i = (C_p)(\rho_m)(V)(St)$$

which upon rearrangement becomes

$$h = \frac{4\ C_p}{\pi D^2}\ (w)(St) \quad .$$

Substituting conversion factors and numerical constants gives the working equation:

$$h = \frac{(4)(3600\ \frac{sec}{hr})}{\pi\ (.062)^2}\ (C_p)(w)(St)$$

or

$$h = 1.192 \times 10^6 \, (C_p)(w)(St) \quad . \tag{49}$$

A sample calculation for the previously used example is:

$$h = (1.192 \times 10^6)(0.846)(1.08)(0.558 \times 10^{-3})$$
$$= 607.7 \text{ Btu/(hr)(ft)(}^\circ\text{F)}$$

Heat Losses

The electrical power input was measured and tabulated. The power transferred to the fluid as measured by temperature rise and flow rate was computed and compared with the electrical power input. For the run 35-1, these are compared as:

Electrical Power = (47.0 volts)(27.0 amps)
= 1270 watts $\pm$ 15 watts,

Input to Fluid = (1.08 lb/sec)(1.233°F)(0.846 Btu/(lb)(°F)(3600 sec/hr)
= 4056 Btu/hr
= 1189 watts,

Power Loss $= \dfrac{(1270 - 1189)(100)}{1270}$
= 6.38% $\pm$ 1.1%.

CHAPTER 6

SUMMARY AND ANALYSIS OF RESULTS

A summary of nominal and measured compositions studied, the range of Reynolds numbers, and the approximate stream temperature are presented in Table 1. Detailed observed and calculated data are presented in Appendix C.

Friction Losses

The pressure drop data was correlated by Nikuradse's friction factor equation for smooth tubes.

$$\frac{1}{\sqrt{f}} = 4.0 \log (Re \sqrt{f}) - 0.40 \tag{30}$$

The friction factors for each run were calculated by the method given in equation (28) and $1/\sqrt{f}$ plotted versus $w\sqrt{f}$ for all of the data. Although the pressure drop measurements were made under non-isothermal conditions, no correction factor was applied. Each run within a series was made at nearly the same bulk temperature (within about 2°F). The viscosity, heat capacity, and thermal conductivity of the fluids were determined at the overall average bulk temperature during the run. Since the power was increased at a proportional rate with the flow rate, any variation due to the wall temperature was incorporated into the values of viscosity which were obtained. The plot of $1/\sqrt{f}$ versus

Table 1

Range of Observed Data

Nominal Composition	Measured Compositions, % Solvent by Volume	Largest Reynolds Number	Average Fluid Temperature, °F
Pure water	——	102,000	71.4
5% solvent in water	4.76-4.49	95,000	70.9
20% solvent in water	19.39-18.20	58,000	71.6
35% solvent in water	34.2	37,000	72.8
50% solvent in water	49.19	17,500	70.6
Pure solvent	100	95,500	72.0

$w\sqrt{f}$ is shown in Figure 10 for the various fluids studied.

The viscosity was calculated by the following equation for each fluid and was plotted versus flow rate as shown in Figure 11.

$$\log\mu = \log w\sqrt{f} - \frac{1}{4\sqrt{f}} + \log 30{,}600 - 0.10 \qquad (30\text{-b})$$

The viscosities given in Figure 11 were used to calculate the Reynolds number and Prandtl number in the analysis of the heat transfer data.

The two lines on Figure 10 for the water and solvent were drawn with a slope of 4.0 in accordance with Nikuradse's equation for Newtonian fluids and the experimental results agree satisfactorily with the lines. Viscosities obtained from these lines agree well with the experimental values for water. The line for pure solvent was obtained by least squares analysis with a slope of 4.0. This line gives a viscosity of 0.95 centipoise for solvent at a temperature of 72°F. This agrees fairly well with the value of 0.97 centipoise measured by Finnigan (16) for the same temperature.

All of the mixtures of solvent in water behave as pseudoplastic fluids approaching Newtonian behavior at high rates of shear. The limiting viscosity at these high rates of shear has been used by several authors to correlate their data throughout the entire turbulent flow

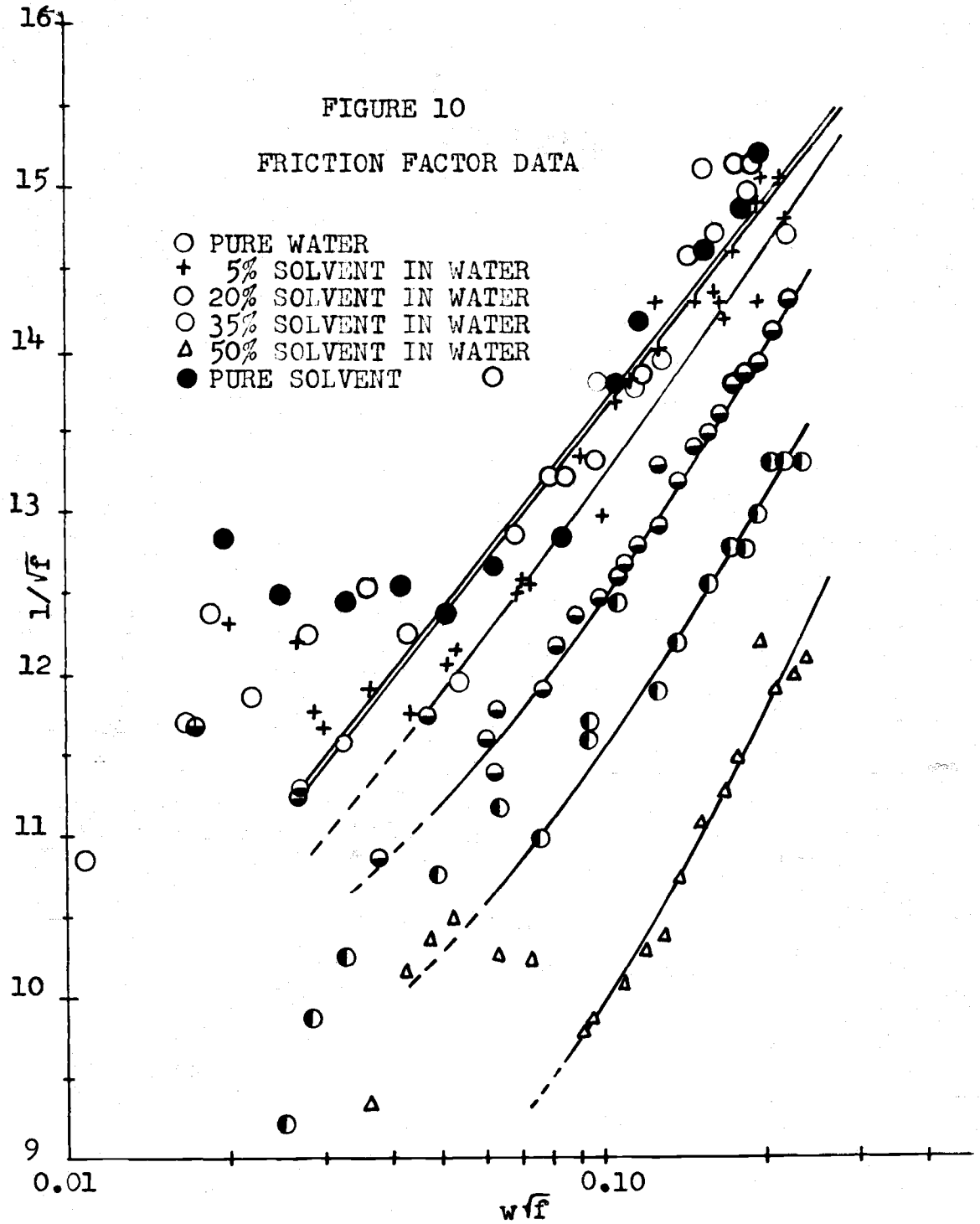
FIGURE 10
FRICTION FACTOR DATA
PURE WATER
5% SOLVENT IN WATER
20% SOLVENT IN WATER
35% SOLVENT IN WATER
50% SOLVENT IN WATER
PURE SOLVENT
16
15
14
13
12
11
10
9
$1/\sqrt{f}$
0.01
0.10
$w\sqrt{f}$

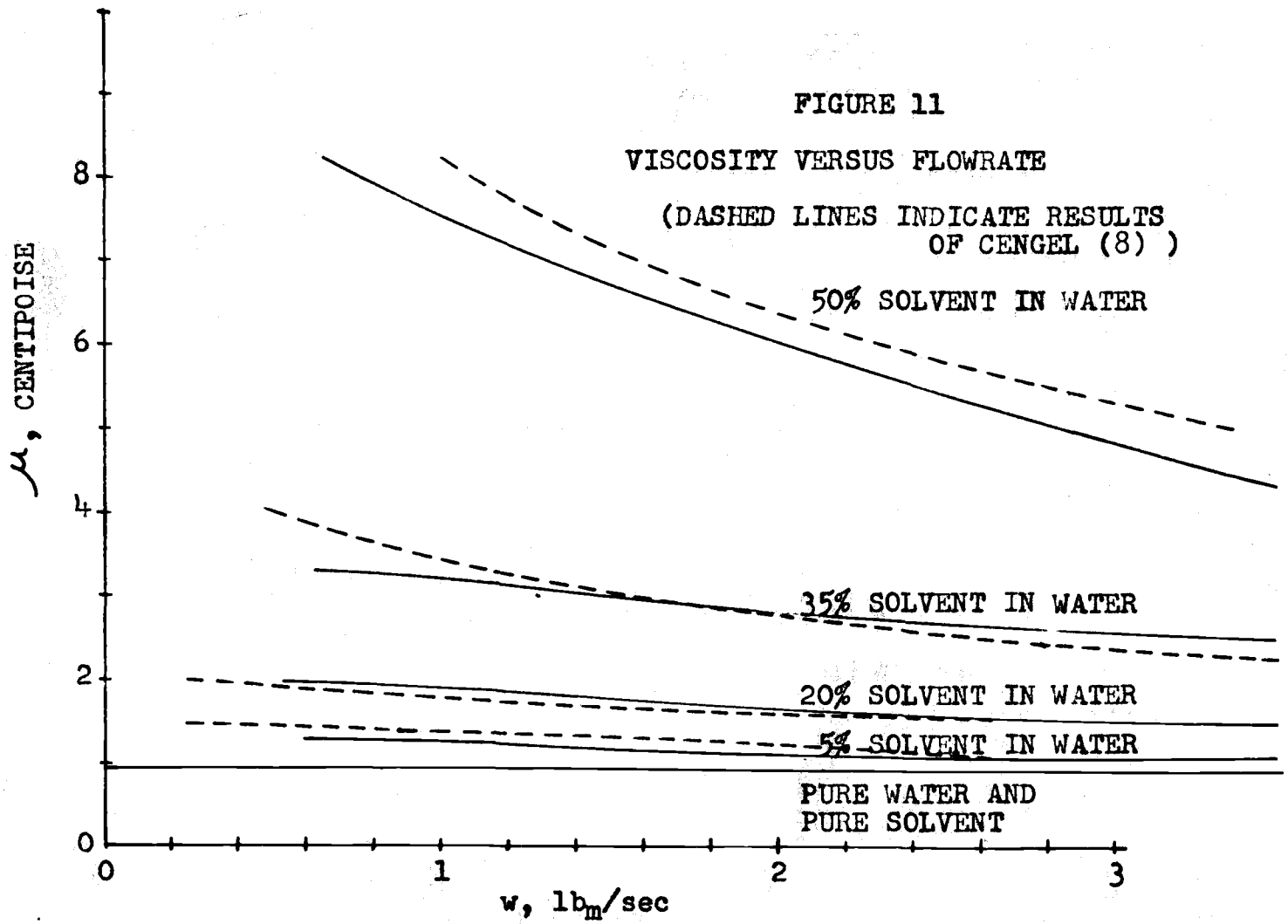

FIGURE 11

VISCOSITY VERSUS FLOWRATE

(DASHED LINES INDICATE RESULTS OF CENGEL (8))

range. The results of this investigation gave a continual change in viscosity with a flow rate for a given composition although all of the measurements were in the turbulent range. The viscosities near the transition zone were erratic and the lines on Figure 10 were extrapolated into this region. The viscosities at the high flow rates tend to approach a constant value.

The broken lines on Figure 11 show the viscosity data obtained independently by Cengel (8) for isothermal flow of the same fluid in the same test section. Good agreement exists between the two sets of data and the viscosity of the dispersions may be predicted within ± 10% by an empirical equation derived by Cengel.

$$\mu_m/\mu_c = 1 + 2.5\phi - 11.01\phi^2 + 52.62\phi^3 \tag{47}$$

Heat Transfer

The heat transfer data was correlated by Colburn's equation.

$$\left(\frac{h}{GC_p}\right)_f \left(\frac{C_p\mu}{k}\right)_f^{2/3} = 0.023 \left(\frac{DG}{\mu}\right)_f^{-0.2} \tag{10}$$

The various properties of the fluid to be used in this equation were found by fitting the data as closely as possible to the equation for single-phase fluids. This was done to determine whether the properties of the mixture,

the continuous phase, or the dispersed phase should be used. It is assumed that heat capacity and density are additive properties and may be calculated knowing the volume and/or weight fractions of the components in the dispersion. In Figure 12 the term St $(C_{p_m}\mu_m)^{2/3}$ was plotted versus Re and compared to the theoretical equations for pure water and solvent. This means of plotting was designed to determine the effect of concentration on the effective thermal conductivity of the dispersion. The heat capacity of the mixture was used and the viscosity determined from Figure 11. The data for water and all the dispersions lie in one group about the line representing Equation (10) for water. The solvent data form another group which also agree with Equation (10) for pure solvent. These results indicate that the effective thermal conductivity of the dispersion during turbulent heat transfer is the conductivity of the continuous phase. Therefore all heat transfer data are plotted in Figure 13 where St $(Pr)^{2/3}$ is plotted versus Re using the thermal conductivity of the continuous phase. The line represents Equation (10). The average deviation of all the data on the dispersions was 14% from the equation. The average deviations of each series of runs from Equation (10) are given in Table 2.

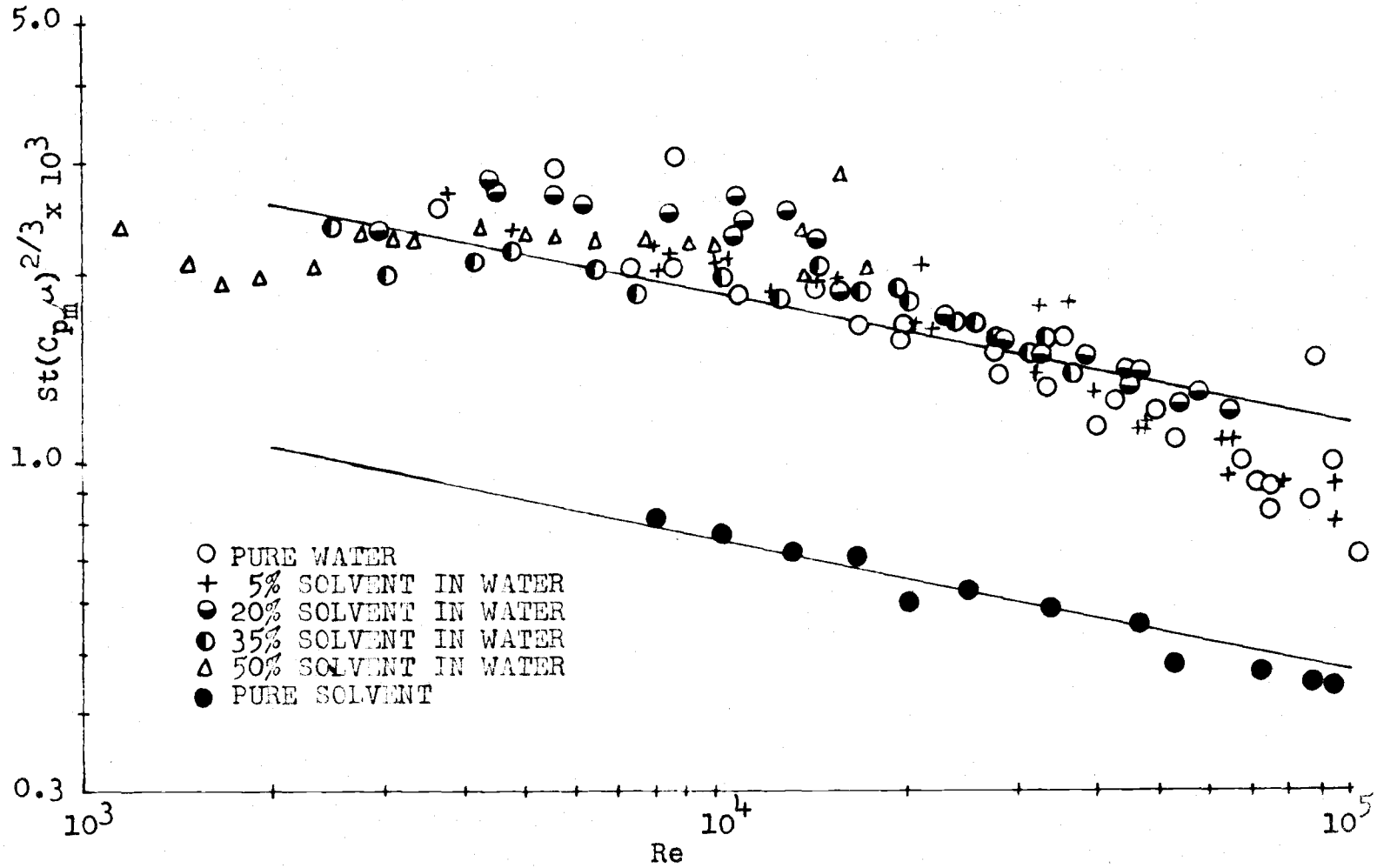

FIGURE 12

EFFECT OF THERMAL CONDUCTIVITY ON HEAT TRANSFER CORRELATION

FIGURE 13

HEAT TRANSFER CORRELATION

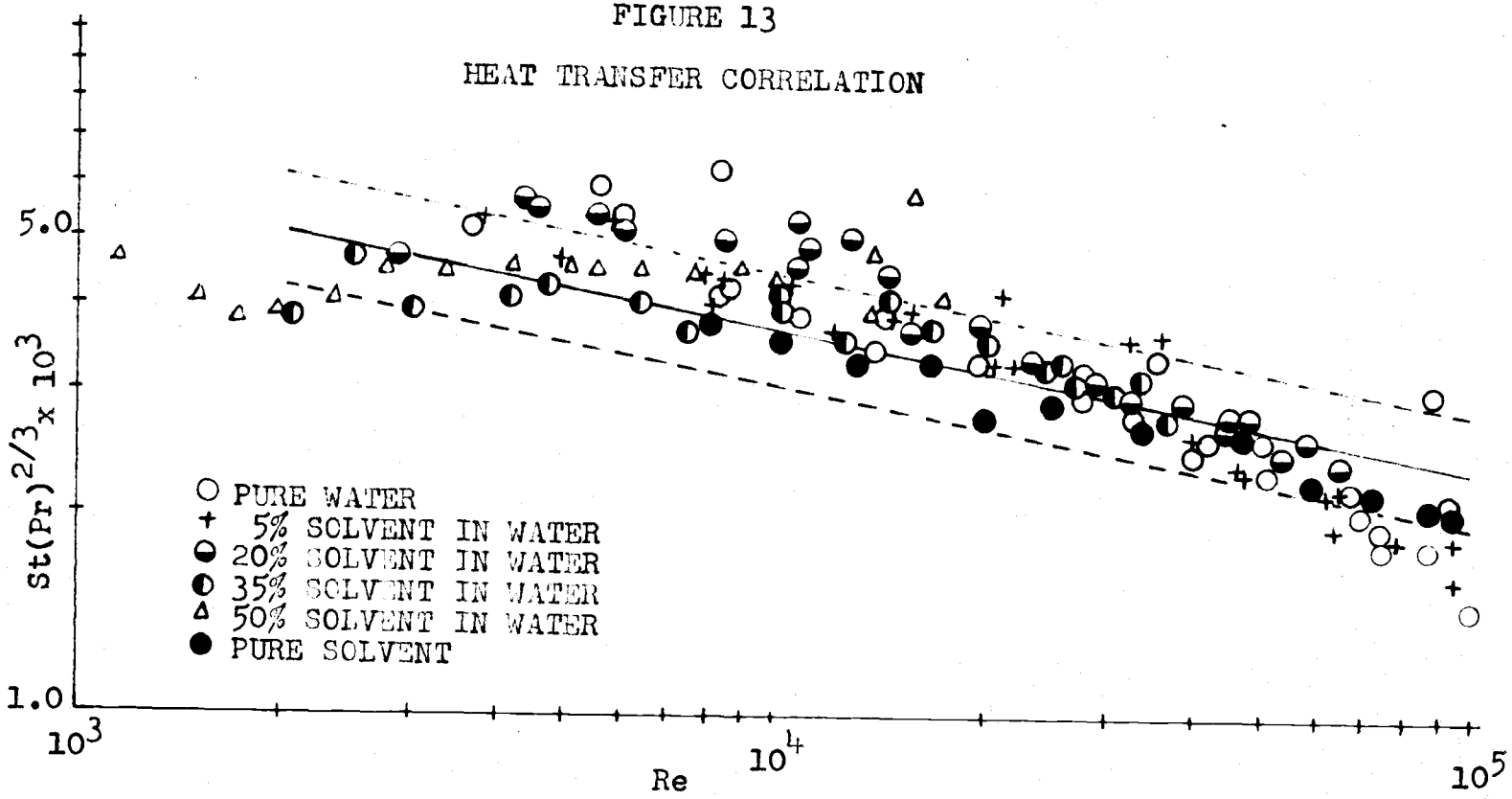

Table 2

Average Per Cent Deviations of the Data from the Theoretically Predicted $St(Pr)^{2/3}$ Group from Equation (10)

Nominal Composition, % by Volume	Per Cent Deviation from Theoretical Values
Pure water	15.0
5% solvent in water	16.0
20% solvent in water	17.0
35% solvent in water	8.0
50% solvent in water	12.0
Pure solvent	9.0
Average of Dispersions	14.0
Overall Average	14.0

The considerable scattering of the heat transfer data is probably due to errors in temperature measurement. There was a small rise in bulk temperature in passing through the test section but the temperatures were measured to 0.01°C so the per cent error is of the order of 1%. Larger errors may be expected in measuring wall temperature; although the thermocouples were accurate to 0.1°F, difficulty in positioning the wall thermocouples in the relatively thin tube wall probably caused considerably larger errors. These errors are magnified since the temperature difference between wall and fluid was usually of the order of 4°F. The wall thermocouples were placed under the heating ribbon and the thermocouple reading could possibly be affected by the ribbon temperature and the high heat flux. Further work is

recommended with a thick-walled tube so that the thermocouples may be placed deeper in the tube wall. Seventy-five per cent of the data shown in Figure 13 lie within ± 20% of the line. The best correlation by Finnigan (16, p. 106) was obtained using the heat capacity of the continuous phase. Miller and Moulton (25, p. 15) and Bonilla, et al. (5, p. 127) used C_{pm} and k_c for their calculations on solid in liquid suspensions. Several other authors have used the thermal conductivity of the medium in their calculations.

The heat transfer coefficient for the inside of the pipe was calculated from Equation (49) and the results are shown in Figure 14. The values of h for water at the high flow rates tend to fall below those predicted from Equation (49).

The electrical power input to the heating coil is tabulated in Appendix C. The heat input used by Finnigan (16) was the electrical input. These values can be compared with the measured power input as tabulated in Appendix C. The average power loss was 6 per cent and the maximum about 13 per cent.

FIGURE 14

HEAT TRANSFER COEFFICIENT VERSUS MASS FLOW RATE

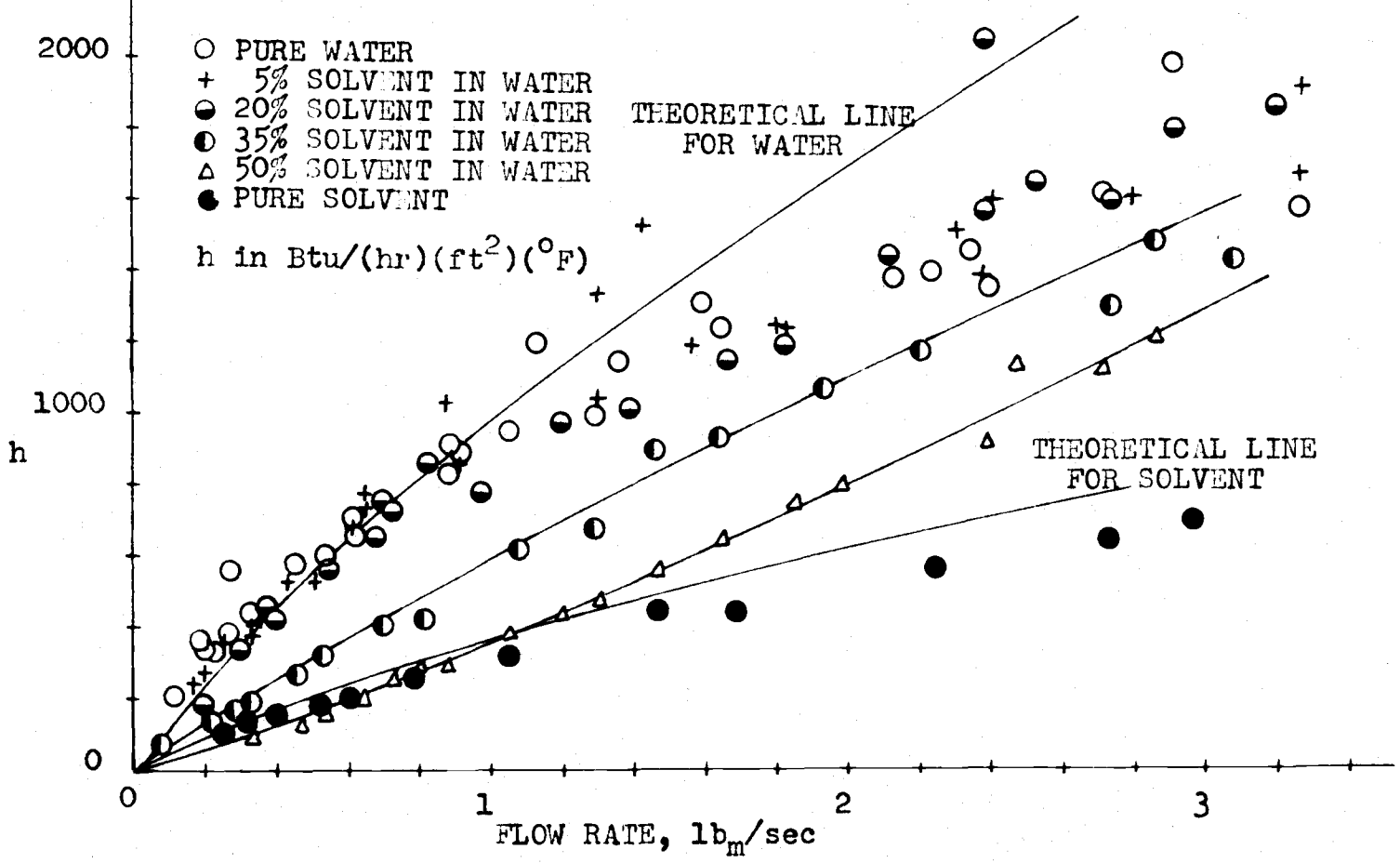

CHAPTER 7

CONCLUSIONS

Apparent viscosities of liquid-liquid dispersions were measured under non-isothermal conditions of turbulent flow in a smooth tube. These turbulent viscosities were calculated by substituting a measured friction factor into Nikuradse's friction factor equation and solving for the viscosity. As the concentration of the dispersed phase (petroleum solvent) increased the viscosity increased. The results agree with an independent study made by Cengel (8) on the same system but under isothermal conditions. The agreement between the two sets of data should be good since the non-isothermal data were obtained at almost the same average bulk temperature as the isothermal data and relatively small temperature differences were employed. His equation is applicable for turbulent flow rates above 1.0 lb/sec with an accuracy of ± 10%. The empirical equation proposed by Cengel to predict turbulent viscosities from composition of the dispersion may be employed to calculate the viscosity term used in subsequent heat transfer correlations.

(47) $$\mu_m/\mu_c = 1 + 2.5\phi - 11.01\phi^2 + 52.62\phi^3$$

Forced convection heat transfer coefficients were measured for turbulent flow in a circular tube for various dispensions and for the pure components.

The heat transfer data were satisfactorily correlated by the following equation:

$$\left[\frac{h}{C_{p_m}G}\right]_{film}\left[\frac{C_{p_m}\mu_m}{k_c}\right]^{2/3} = 0.023\left[\frac{DG}{\mu_m}\right]^{-0.2} . \tag{10}$$

The heat capacity was the weighted average of the two components; the apparent viscosity was calculated from Figure 11 and the thermal conductivity of the continuous phase gave the best results. All data show an average deviation of 14% from the equation.

The heat transfer coefficients of the dispersions were intermediate between those for the pure solvent and pure water. The 5% and 20% solvent in water dispersions had very nearly the same heat transfer coefficient as that for pure water.

CHAPTER 8

RECOMMENDATIONS FOR FURTHER WORK

The results obtained in this thesis give a good correlation for turbulent flow pressure drop and heat transfer for a liquid-liquid dispersion flowing in a circular tube. During this investigation, many ideas were formed on further work which could be done. Some of the specific recommendations are given below:

(1) The investigation of other pairs of immiscible liquids. These liquids could have similar densities but widely different heat transfer coefficients or widely differing viscosities.

(2) The use of a heavy wall tube. The embedding of the thermocouples deep in the wall and covered with an electrically insulating material to permit more accurate measurements of the wall temperature.

(3) The use of various length and diameter tubes to determine the effects of settling during the passage of the fluid through the horizontal section.

CHAPTER 9

BIBLIOGRAPHY

1. Alves, George E., D. F. Boucher, and R. L. Pigford. Pipe-line design for non-Newtonian solutions and suspensions. Chemical Engineering Progress 48: 388-393. 1952.

2. _____. Flow of non-Newtonian suspensions. Chemical Engineering 56:107-109. May 1949.

3. Becher. Paul. Emulsions: theory and practice. New York, Reinhold, 1957. 382 p.

4. Beckers, H. L., Heat transfer in turbulent tube flow. Applied Science Research 6:147-190. 1956.

5. Bonilla, Charles F. et al. Heat transfer to slurries in pipe: chalk and water in turbulent flow. In: Chemical Engineering Progress Symposium Series no. 5, vol. 49. New York, American Institute of Chemical Engineers, 1953. p. 127-135.

6. Butler, J. B. School of Mines and Metallurgy, 1926. 62 p. (University of Missouri. Bulletin Technical Series 9, no. 4)

7. Caldwell, D. H. and H. E. Babbitt. The flow of muds, sludges, and suspension in a circular pipe. American Institute of Chemical Engineers Transactions 37:257. April 25, 1941.

8. Cengel, John A. Viscosity of liquid-liquid dispersions in laminar and turbulent flow. Master's thesis. Corvallis, Oregon State College, 1959. 110 numb. leaves.

9. Clayton, William. The theory of emulsions and their technical treatment. 3d ed. New York, Blakiston, 1953. 458 p.

10. Colburn, Allan P. A method of correlating forced convection heat transfer data and a comparison with fluid friction. American Institute of Chemical Engineers Transactions 29:174. 1933.

11. Dittus, F. W. and L. M. K. Boelter. Heat transfer in automobile radiators of the tubular type. University of California Publications in Engineering 2:443-461. October 17, 1930.

12. Dix, F. Johnson and G. W. Scott Blair. On the flow of suspensions through narrow tubes. Journal of Applied Physics 11:574. September 1940.

13. Drew, Thomas B., E. C. Koo, and W. H. McAdams. The friction factor for clean round pipes. American Institute of Chemical Engineers Transactions 28:56-72. 1932.

14. Drew, Thomas B. and John W. Hoopers, Jr. Advances in chemical engineering. New York, Academic Press, 1956. 448 p.

15. Farbar, Leonard and Morgan J. Morley. Heat transfer to flowing gas-solids mixtures in a circular tube. Industrial and Engineering Chemistry 49:1143-1150. July 1957.

16. Finnigan, Jerome W. Pressure losses and heat transfer for the flow of mixtures of immiscible liquids in circular tubes. Ph.D. thesis. Corvallis, Oregon State College, 1958. 154 numb. leaves.

17. Hatschek, Emil. Die Viskosität von Blutkörperchen-Suspensionen. Kolloid-Zeitschrift 27:163-165. 1920.

18. von Karman, T. Mechanical similitude and turbulence. National Advisory Committee for Aeronautics. Technical Memorandum no. 611. 1931.

19. Knudsen, James G. and Donald L. Katz. Fluid dynamics and heat transfer. New York, McGraw-Hill, 1958. 576 p.

20. Kunitz, M. An empirical formula for the relation between viscosity of solution and volume of solute. Journal of General Physiology 9:715-725. 1926.

21. McAdams, William H. Heat transmission. 3d ed. New York, McGraw-Hill, 1954. 532 p.

22. McAdams, William H. and T. H. Frost. Heat transfer for water flowing in pipes. Chemical and Metallurgical Engineering 30:234-236. February 11, 1924.

23. _____. Heat transfer for water flowing inside pipes. Refrigerating Engineering 10:323-334. March 1924.

24. Metzner, A. B., R. D. Vaughan, and G. L. Houghton. Heat transfer to non-Newtonian fluids. American Institute of Chemical Engineers Journal 3:92-100. March 1957.

25. Miller, Aven P. and R. W. Moulton. Heat transfer to liquid-solid suspensions in turbulent flow in pipes. Trend in Engineering at the University of Washington 8:15-21. April 1956.

26. Morris, F. H. and Walter G. Whitman. Heat transfer for oils and water in pipes. Industrial and Engineering Chemistry 20:234-240. March 1928.

27. Oliver, D. R. and Stacey G. Ward. Relationship between relative viscosity and volume concentration of stable suspensions of spherical particles. Nature 171:396-397. 1953.

28. Orr, Clyde, Jr. and J. M. DallaValle. Heat transfer properties of liquid-solid suspensions. In: Chemical Engineering Progress Symposium Series no. 9, vol. 50. New York, American Institute of Chemical Engineers, 1954. p. 29-45.

29. Perry, John H. (ed.). Chemical engineers' handbook. 3d ed. New York, McGraw-Hill, 1950. 1942 p.

30. Richardson, E. G. The flow of emulsions. II. Journal of Colloid Science 8:367-373. 1953.

31. Russell, T. W. F., G. W. Hodgson, and G. W. Govier. Horizontal pipe-line flow of mixtures of oil and water. Canadian Journal of Chemical Engineering 37:9-17. February 1959.

32. Salamone, Jerome J. and Morris Newman. Heat transfer design characteristics: water suspension of solids. Industrial and Engineering Chemistry 47:283-288. 1955.

33. Sherwood, T. K. and J. M. Petrie. Heat transmission to liquids flowing in pipes. Industrial and Engineering Chemistry 24:736-745. 1932.

34. Sieder, E. N. and G. E. Tate. Heat transfer and pressure drop of liquids in tubes. Industrial and Engineering Chemistry 28:1429-1435. 1936.

35. Slawecki, T. K. and M. C. Molstad. Thermal conductivity of water, glycols, and glycol ethers. Industrial and Engineering Chemistry 48:1100-1103. 1956.

36. Sleicher, C. A. Jr. and M. Tribus. Heat transfer in a pipe with turbulent flow and arbitrary wall-temperature distribution. American Society of Mechanical Engineers Transactions 79:789-797. 1957.

37. Smith, J. F. Downie. Heat transfer and pressure drop data for an oil in a copper tube. American Institute of Chemical Engineers Transactions 31:83-112. November 1934.

38. Smith, R. A. Experiments on the flow of sand-water slurries in horizontal pipes. Institute of Chemical Engineers Transactions (London) 33:85-92. 1955.

39. Spells, K. E. Correlations for use in transport of aqueous suspensions of fine solids through pipes. Institute of Chemical Engineers Transactions (London) 33:79-84. 1955.

40. Stanton, T. E. and J. R. Pannell. Similarity of motion in relation to the surface friction of fluids. Philosophical Transactions of the Royal Society (London) 214A:199-224. 1914.

41. Taylor, G. I. The viscosity of a fluid containing small drops of another fluid. Royal Society of London Proceedings 138A:41-48. 1932.

42. Van der Held, E. F. M. and F. G. Van Drunen. Physica 55:865. 1949.

43. Wang, R. H. and James G. Knudsen. Thermal conductivity of liquid-liquid emulsions. Industrial and Engineering Chemistry 50:1667-1670. 1958.

44. Winding, C. C., G. P. Baumann, and W. L. Kranich. Flow properties of pseudo-plastic fluids. Chemical Engineering Progress 43:527-529. 1947.

APPENDICES

APPENDIX A

NOMENCLATURE

Many of the equations in this paper involve dimensionless ratios, and any consistent system of units might be used. The units given below are those chosen by the author for this work.

Latin Letter Symbols

Symbol	Meaning	Units
A	Cross sectional area of flow channel	ft^2
A'	Surface area of wall of flow channel	ft^2
b	Manometer reading	ft
C_o	Orifice discharge coefficient	
C_p	Specific heat at constant pressure	$\frac{Btu}{(lb_m)(^oF)}$
D	Inside diameter of tube	ft
D_1	Inside diameter of pipe	ft
D_o	Diameter of orifice	ft
d	Diameter of particle in dispersed phase	ft
e	Base of natural logarithms	
F	Frictional resistance force at wall of conduit	lb_f
f	Fanning friction factor	

Symbol	Meaning	Units
G	Mass velocity	$\frac{lb_m}{(ft^2)(sec)}$
g	Gravitational acceleration	$\frac{ft}{sec^2}$
g_c	Conversion constant = 32.174	$\frac{(lb_m)(ft)}{(lb_f)(sec^2)}$
h	Film heat transfer coefficient	$\frac{Btu}{(hr)(ft^2)(^oF)}$
K	Constant in orifice equation	
k	Thermal conductivity	$\frac{Btu}{(hr)(ft)(^oF)}$
L	Length of conduit	ft
L'	Vertical distance between orifice pressure taps	ft
l	Length between thermocouples	in.
n	Constant on heat transfer equation	
n'	Flow behavior index	
P	Static pressure	$\frac{lb_f}{ft^2}$
Q	Power input to heater coil	watts
q	Steady state heat transfer rate	$\frac{Btu}{hr}$
t	Temperature	^oF
t_b	Temperature of flowing fluid	^oF
t_w	Temperature of tube wall under heating coil	^oF

Symbol	Meaning	Units
V	Average linear velocity of fluid	$\frac{ft}{sec}$
U'	Overall heat transfer coefficient	$\frac{Btu}{(hr)(ft)(^oF)}$
w	Mass flow rate	$\frac{lb_m}{sec}$
$\overline{W}$	Work done by flowing fluid	$\frac{(ft)(lb_f)}{lb_m}$
X	Volume fraction	
x	Weight fraction	
Z	Height above a datum plane	ft

Greek Letter Symbols

α	Correction factor in expression for kinetic energy of fluid	
α	A function of, used in correlating dimensionless quantities	
γ	Fluid consistency	$\frac{lb_m}{(ft)(sec)^{2-n'}}$
Δ	Finite difference	
θ	Constant in some equations	
μ	Dynamic viscosity	Centipoise
μ_c	Viscosity of continuous phase	Centipoise
μ_d	Viscosity of dispersed phase	Centipoise
μ_m	Apparent viscosity of mixture	Centipoise
π	Constant, 3.1416 ...	
ρ	Density	$\frac{lb_m}{ft^3}$

Symbol	Meaning	Units
σ	Conversion factor, 1488	$\frac{c.p.}{(lb_m)(ft)(sec)}$
τ	Shear stress	$\frac{lb_f}{ft^2}$
ϕ	Volume fraction of dispersed phase	
ψ	Function of undetermined form in expression for heat transfer coefficient	

Composite Symbols

BWG	Birmingham wire gauge	
gpm	U.S. gallons per minute	$\frac{gal}{min}$
log	Common logarithm (base 10)	
$\overline{lW}$	Lost work due to friction in a flowing fluid	$\frac{(ft)(lb_f)}{lb_m}$
$Nu = \frac{hD}{k}$	Nusselt number	
$Pr = \frac{C_p \mu}{k}$	Prandtl number	
$Re = \frac{DG}{\mu}$	Reynolds number	
$St = \frac{h}{C_p G}$	Stanton number	
ΔP	Pressure difference between two points in a flowing fluid	$\frac{lb_f}{ft^2}$

Symbol	Meaning	Units
ΔP_f	Pressure difference due to fluid friction	$\frac{lb_f}{ft^2}$

Subscripts

b	Bulk, the flowing fluid
c	Continuous phase
d	Dispersed phase
e	Effective
f	Force (as in lb_f), or friction (as in P_f), or film
m	Mass (as in lb_m), or mixture
o	Orifice
w	Tube wall under heating coil
1, 2	Refer to positions in a flowing system

APPENDIX B

PROPERTIES OF PURE LIQUIDS AND CALIBRATION CURVES

The solvent used as the organic component of the pair of immiscible liquids in this investigation was a commercial cleaning solvent manufactured by the Shell Oil Company under the name "Shellsolv 360". This liquid is clean and colorless, and is readily available in 55 gallon drum quantities at reasonable cost. The properties of this solvent are presented in Table 3.

Table 3

Properties of "Shellsolv 360"
(Data from Company Specifications)

Gravity, API, 60°F	49.1
Specific Gravity, 60/60°F	0.7835
Color, Saybolt	26+
Flash Tag, O.C., °F	110
Flash Tag, C.C., °F	103
Aromatics, Stoddard, % v	2
A.S.T.M. Distillation, °F:	
Initial Boiling Point	304
Final Boiling Point	362
10% Recovered	317
50% Recovered	323
90% Recovered	342
% Recovered	98.5

Table 3 indicates that the solvent is low in aromatic hydrocarbon content and a fairly high paraffinic content (16, p. 130). Finnigan decided the composition was in the nonane-decane range. He also estimated that the molecular weight was about 134.

The solubilities of hydrocarbons in water are quite low and Finnigan estimated a solubility of 0.05 mole per cent water in petroleum solvent at 70°F. This system consists of a pair of practically immiscible liquids.

Density

The densities of the water, mercury, carbon tetrachloride, and solvent change slightly with a change in temperature. The values used were taken from the Chemical Engineers' Handbook (29, p. 175) and the measurements made by Finnigan (16, p. 132). The specific gravity of the carbon tetrachloride was determined by weighing the volume delivered from a buret. The iodine coloring used had no effect on the specific gravity. The densities of water and solvent are plotted versus temperature in Figure 15. The effective densities of mercury under water and carbon tetrachloride under water are given in Figure 16.

Specific Heat

The specific heat of the petroleum solvent was measured by Finnigan (16, p. 134) and a value of 0.472 Btu/(lb_m)(°F)

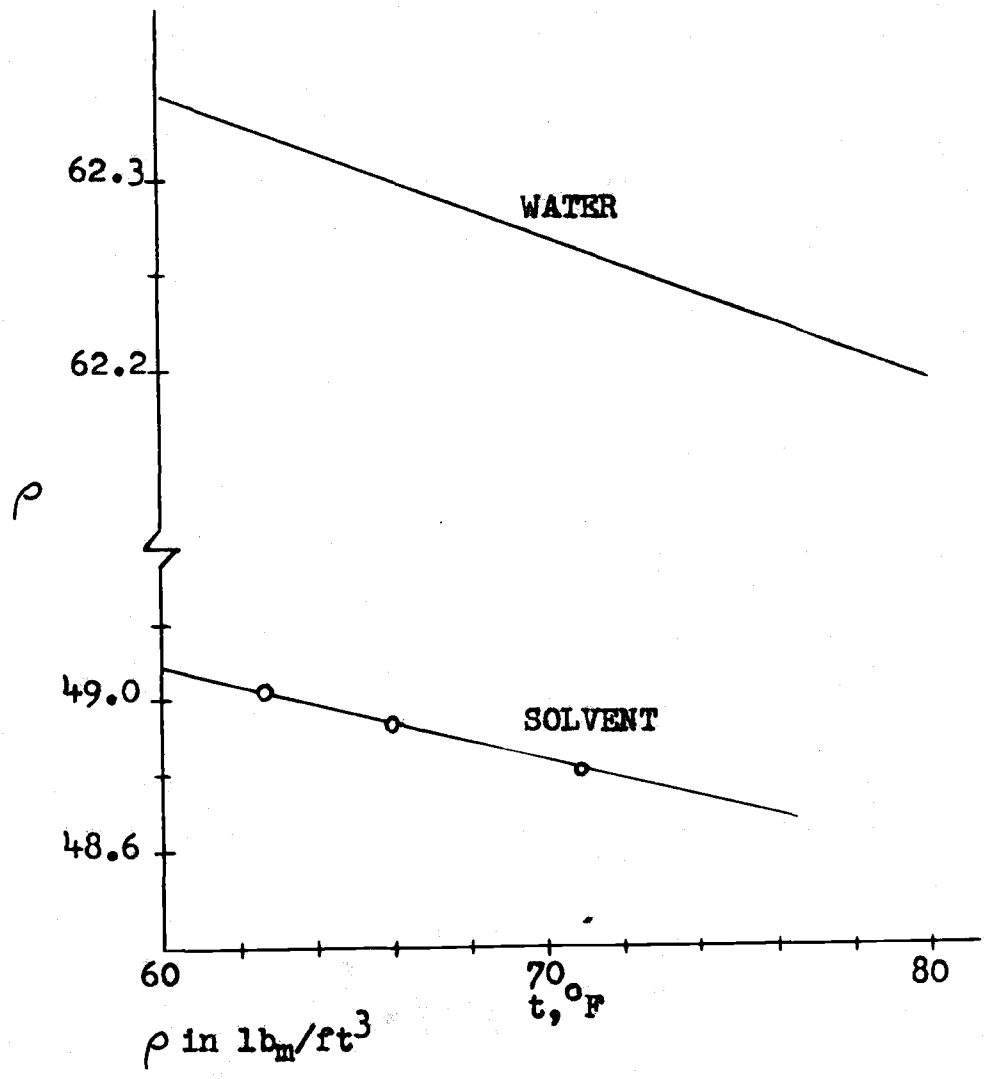

FIGURE 15

DENSITY OF WATER AND SOLVENT VERSUS TEMPERATURE

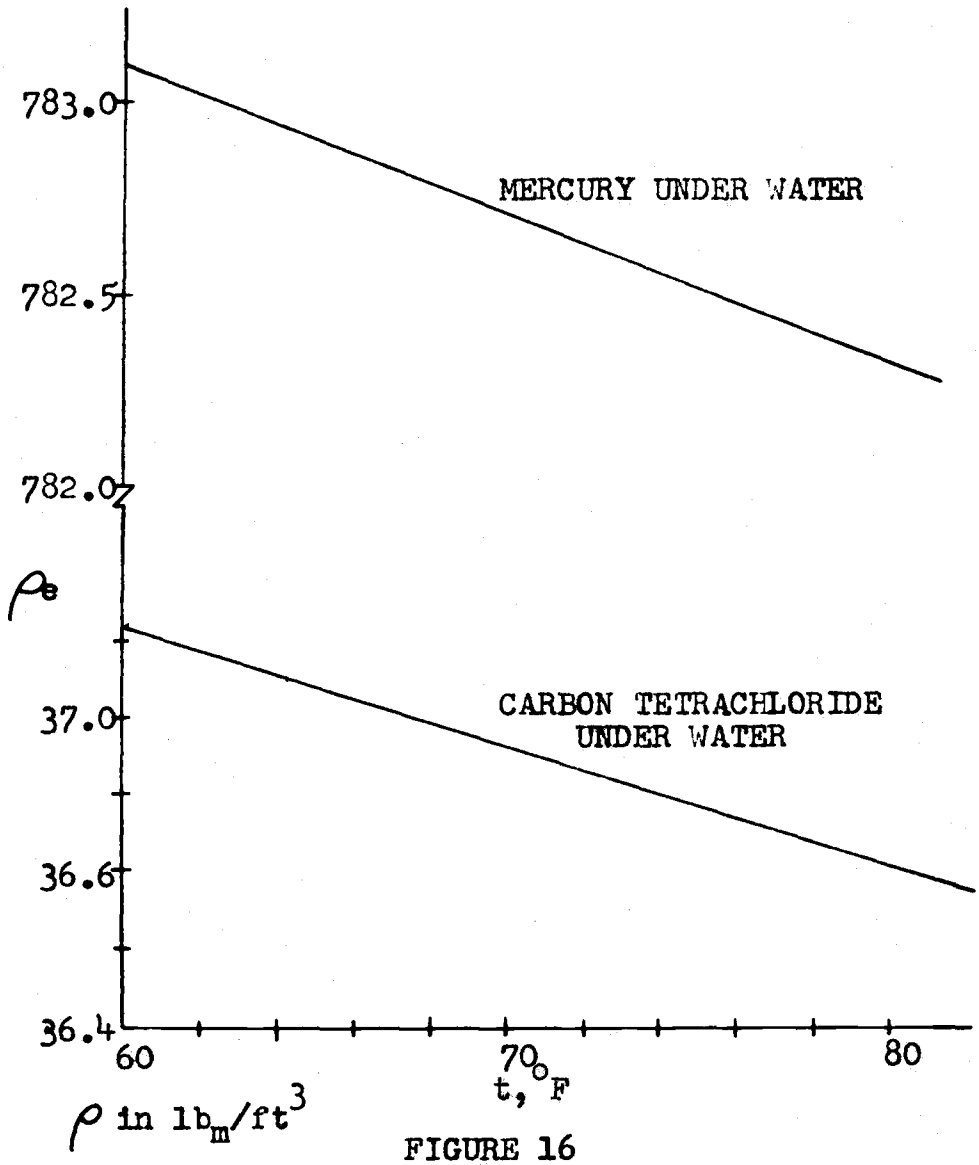

FIGURE 16

EFFECTIVE DENSITY OF MANOMETER FLUIDS

VERSUS TEMPERATURE

at 79°F was measured. Using the known variation of heat capacity with temperature, the value of 0.468 Btu/(lb_m)(°F) was obtained at 71°F. The variation with temperature was small and the value of 0.468 Btu/(lb_m)(°F) was used throughout the present work.

The specific heat of water is 1.0 Btu/(lb_m)(°F) ± 0.1 per cent between 50 and 80°F and this value was used in all of the calculations.

Thermal Conductivity

Wang (43, p. 1667) has measured the thermal conductivity of a petroleum solvent with properties practically identical to those of the solvent used in this investigation. The thermal conductivity of hydrocarbon mixtures change slowly with changes in composition at a given temperature and Wang's values were applied to the present work.

The thermal conductivity of water is given by McAdams (21, p. 864), Van der Held and Van Drunen (42, p. 865), and the Chemical Engineers' Handbook (29, p. 459).

The thermal conductivity of water and solvent are plotted versus temperature in Figure 17.

Viscosity

The dynamic viscosity of the petroleum solvent was

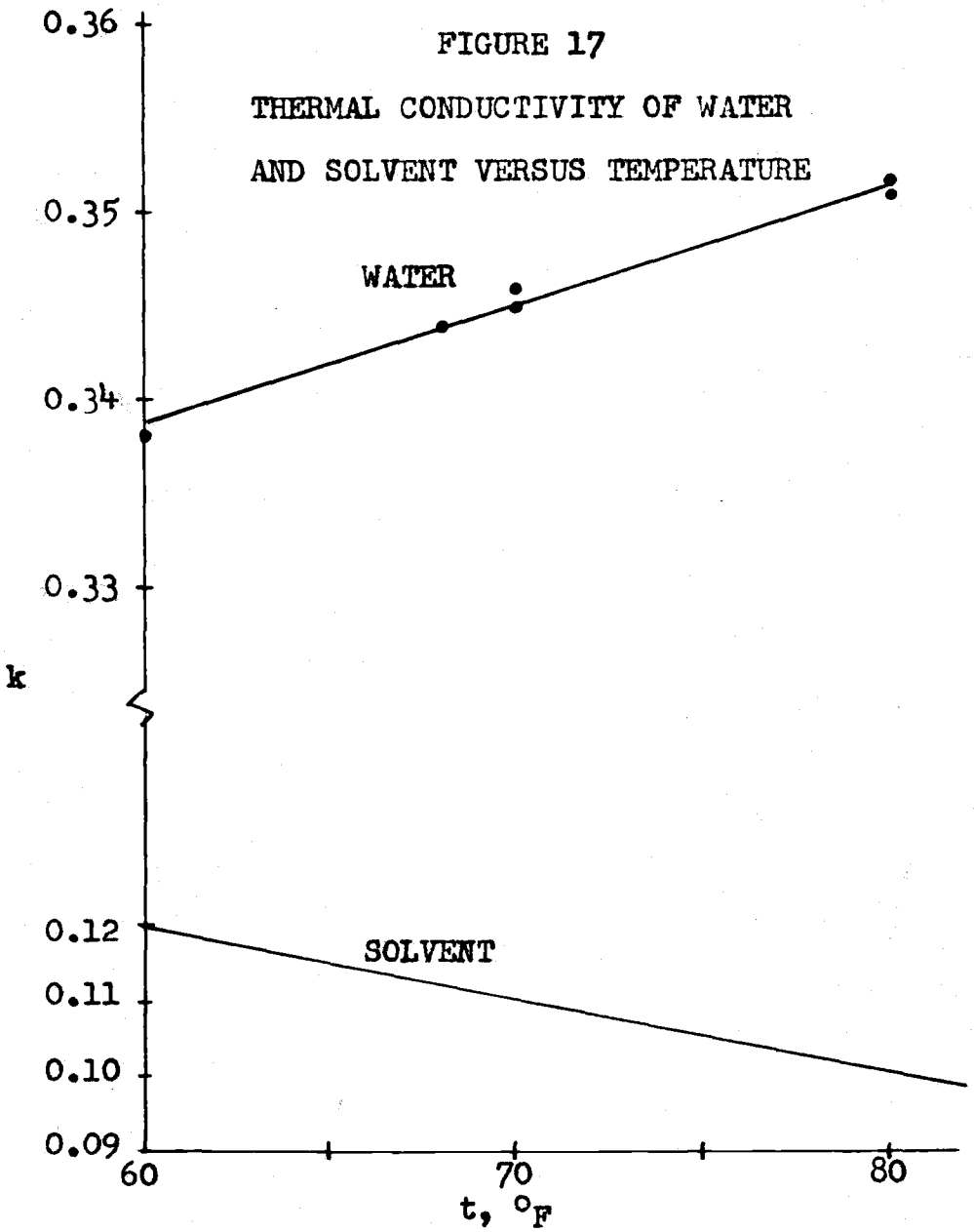

FIGURE 17

THERMAL CONDUCTIVITY OF WATER AND SOLVENT VERSUS TEMPERATURE

k in Btu/(hr)(ft)(°F)

measured in an Ostwald viscometer by Finnigan (16, p. 140). He found a very slight change in viscosity after the solvent had been used several times. The values of viscosity versus temperature are plotted in Figure 18.

The values for the variation of the viscosity of water with temperature (29, p. 374) were obtained from literature values and plotted in Figure 18.

Thermocouples

The thermocouples were calibrated by graphing the temperature measured on the previously standardized Beckman thermometers versus the millivolt readings of the thermocouples during several isothermal runs on pure water. The differences between the various thermocouple readings was negligible and the same calibration curve was used for all thermocouples. The calibration curve is presented in Figure 19.

Orifice Calibration Curve

The orifice calibration curve, as given by Finnigan (16, p. 96) and used in the present calculations, is shown in Figure 20.

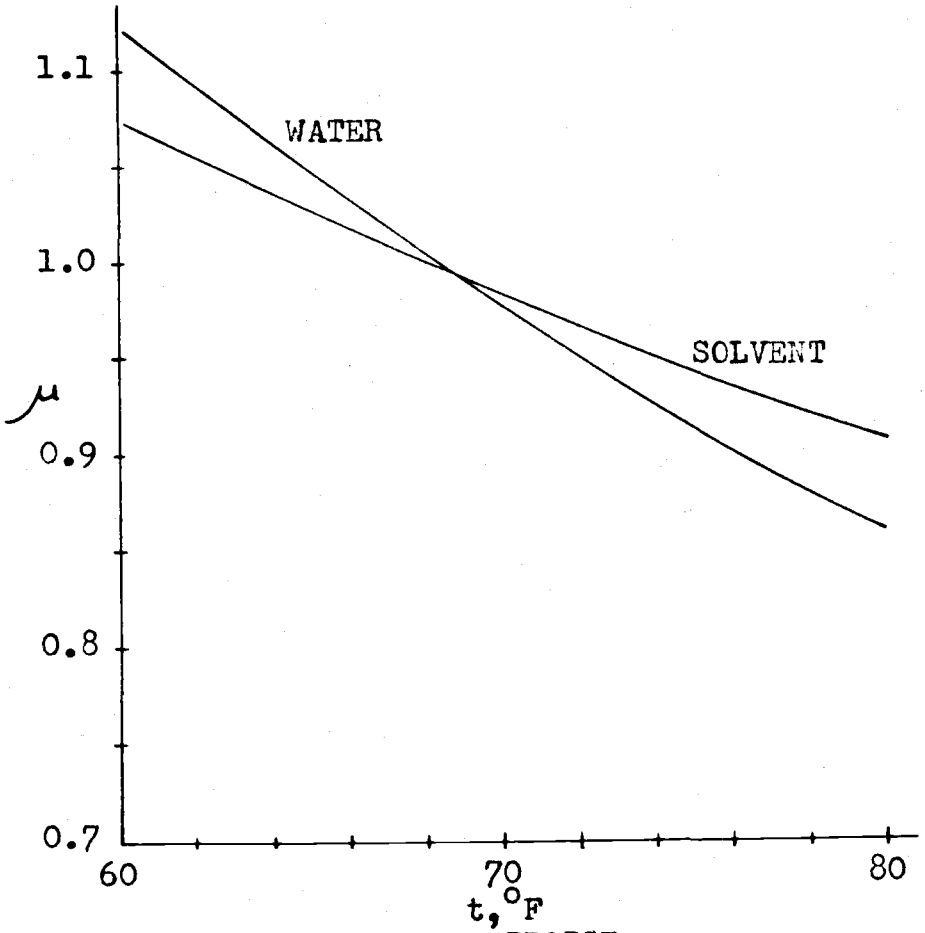

μ, VISCOSITY IN CENTIPOISE

FIGURE 18

VISCOSITY OF WATER AND SOLVENT

VERSUS TEMPERATURE

FIGURE 19

THERMOCOUPLE CALIBRATION CURVE

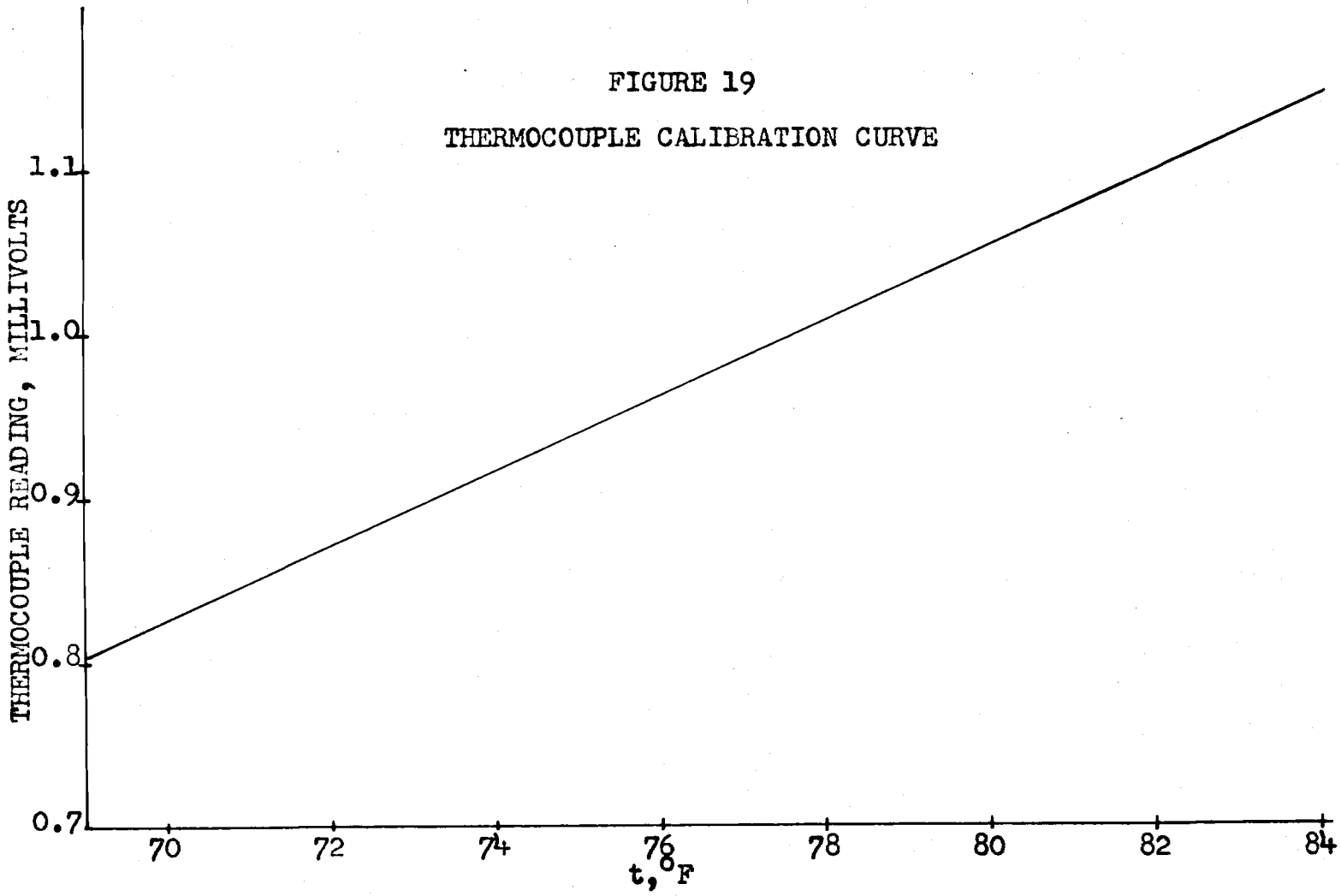

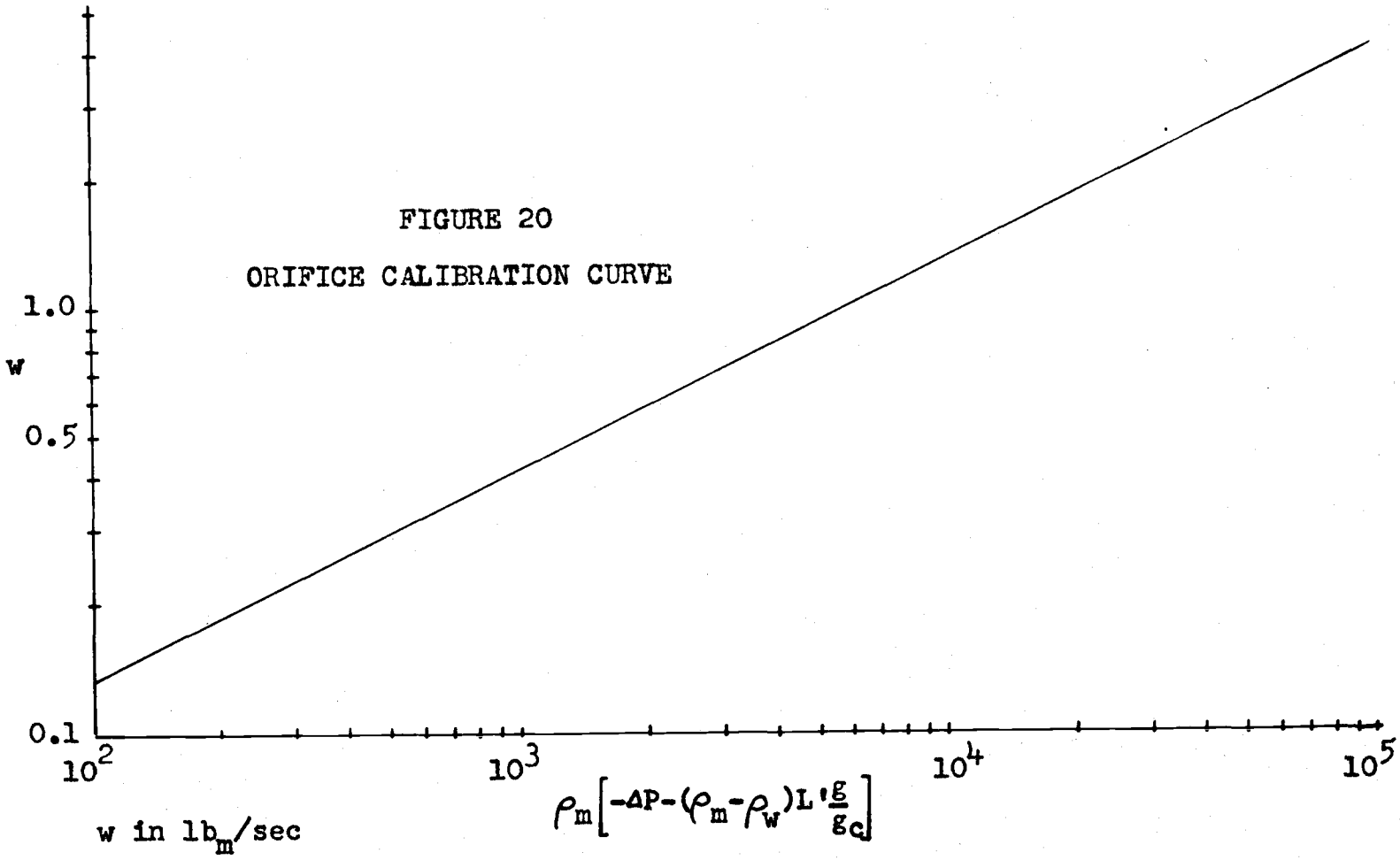

FIGURE 20

ORIFICE CALIBRATION CURVE

APPENDIX C

TABULATED DATA

Table 4

Observed Data

(1)* Run No.	(2) Entering Temp., r_1	(3) Air t, °F	(4) Wall temperature readings t_1, °F	(5) t_2, °F	(6) t_3, °F	(7) t_4, °F
W-1	71.69		71.33	71.60	76.56	77.99
2	70.66		70.37	70.65	75.55	77.99
3	70.16	78.0	70.12	70.43	76.28	79.67
4	70.75	78.0	70.60	70.70	74.85	77.55
5	71.67		71.37	71.99	75.86	79.44
6	71.65		71.22	71.86	76.14	79.00
7	71.46	75.3	71.00	71.17	74.80	77.01
8	71.13	75.2	70.17	70.88	73.98	76.56
9	69.76	74.9	68.76	69.07	73.05	75.34
10	70.20	77.7	68.80	69.51	73.10	76.40
11	69.43	71.9	67.07	68.84	76.80	85.00
12	69.44	77.6	67.88	68.27	73.65	77.13
13	70.02	77.7	67.60	68.27	72.60	75.06
14	71.51	76.1	71.04	71.68	76.88	80.07
15	70.21	77.7	70.13	70.52	73.70	75.90
16	70.78	80.0	70.38	70.66	74.45	76.65
17	70.89	82.1	70.38	70.96	74.96	77.41
18	68.97	78.2	67.74	68.18	72.02	74.80
19	71.13	83.9	71.32	71.68	76.00	78.91
20	69.71	85.7	69.73	71.32	79.18	83.70
21	72.64	78.6	71.95	73.05	80.27	84.81
22	72.90	77.7	71.55	71.86	76.79	80.17
23	70.50	90.0	70.43	70.65	74.36	75.55
24	69.95	92.9	69.95	70.25	73.89	74.89
25	69.86	93.6	69.90	70.04	73.65	75.25
26	70.03	93.6	70.17	70.30	74.23	75.90
27	70.90	94.2	71.27	71.33	76.52	79.23
5-1	70.51	82.7	68.80	69.39	74.10	76.43
2	70.36	79.4	68.18	68.64	72.73	73.05
3	70.33	79.9	67.92	68.36	72.30	74.85
4	71.14	79.7	68.64	69.02	73.65	76.48
5	70.64	74.9	67.30	68.18	73.05	75.69
6	71.03	70.2	70.00	68.84	75.90	79.32

* The run number code is as follows: the first number (or symbol) represents the nominal composition and the second number represents the run number within the series. Thus, W-1 is the first water run, 50-2 is the second run with 50 per cent solvent in water, etc.

Table 4 - Continued

Observed Data

(1)* Run No.	(8) t_5, °F	(9) t_6, °F	(10) t_7, °F	(11) t_8, °F	(12) t_9, °F
	Wall temperature readings				
W-1	77.23	78.11	82.10	75.11	73.89
2	76.56	77.76	81.89	74.28	72.52
3	77.45	78.70	84.60	74.36	72.48
4	75.25	76.43	82.59	72.60	71.73
5	76.48	77.45	84.81	73.70	72.39
6	77.01	78.11	83.58	74.36	73.05
7	75.56	76.40	80.70	73.48	72.35
8	74.58	75.42	81.45	72.39	71.45
9	73.84	74.40	80.88	71.27	69.90
10	73.62	74.36	84.15	70.60	69.68
11	85.12	86.32	90.4	80.93	75.81
12	77.22	78.16	81.89	74.58	71.82
13	74.93	76.00	79.18	72.82	70.84
14	78.60	79.53	86.37	75.47	73.58
15	74.05	74.58	82.29	71.55	70.52
16	74.85	75.51	83.35	72.16	71.13
17	75.60	76.24	84.24	72.56	71.17
18	75.16	76.24	78.39	73.40	71.17
19	76.65	77.45	90.2	73.15	72.12
20	83.35	85.08	91.0	79.44	79.44
21	84.37	85.65	92.0	80.70	77.55
22	77.86	78.74	93.4	74.63	73.75
23	74.93	75.60	82.63	72.82	71.64
24	74.10	74.36	82.34	72.20	70.84
25	74.45	74.68	85.21	71.27	70.60
26	74.23	75.02	86.56	71.50	71.04
27	79.18	79.95	85.79	76.09	74.02
5-1	74.85	75.51	84.19	71.77	70.48
2	73.80	73.98	84.60	70.43	69.51
3	73.00	73.05	83.75	70.04	69.51
4	74.23	74.54	88.0	70.75	69.81
5	75.16	75.64	81.68	71.73	70.37
6	78.60	79.68	86.36	75.51	72.44

Note = Temperatures above 87°F and all air temperatures are given only to the nearest 0.1°F.

Table 4 - Continued

Observed Data

(1)* Run No.	(13) Orifice mm CCl_4	(14) Manometer mm H_g	(15) Test Section Manometer mm CCl_4	(16) mmH_g	(17) Q=IE, watts
W-1	217	10	166	8	1075
2	150	8	118	7	1037
3	329	16	247	12	1612
4		100		59	1850
5		198		100	2223
6	600	40		26	1672
7		29	360	18	1222
8		163		88	1604
9		46	655	30	1523
10		292		148	2383
11	10		10		842
12	29	1	24	2	724
13	55	3	45	2	724
14	297	14	221	10	1548
15		185		98	1767
16		93		55	1778
17		65		40	1767
18	19		15		445
19		259		133	2842
20	42		31		1264
21	53		43		1278
22		308		153	3152
23	607	28	421	20	1191
24		61		39	1391
25		206		110	1920
26		386		204	2243
27	85	4	70	4	995
5-1		42		29	1824
2		166		92	2188
3		239		130	2188
4		311		160	2862
5	324	15	250	12	1348
6	94	4	77	4	1353

(1)*	(2)	(3)	(4)	(5)	(6)	(7)
5-7	70.05	74.3	67.47	68.55	75.16	78.91
8	70.40	71.6	69.07	69.73	75.06	77.81
9	69.97	73.6	69.15	69.60	74.19	76.88
10	70.07	70.0	69.07	69.63	74.76	77.63
11	69.26	81.1	69.15	71.27	77.27	90.2
12	69.17	80.6	68.84	69.51	74.14	77.81
13	68.95	80.8	68.55	68.84	72.60	74.80
14	68.81	82.3	68.31	68.31	71.64	73.15
15	69.04	81.7	68.36	68.68	72.25	73.98
16	69.09	80.3	67.96	68.18	72.12	74.36
17	69.02	81.5	69.07	69.39	73.28	75.60
18	69.14	82.1	69.47	69.47	73.28	75.55
19	69.55	82.9	69.68	69.90	73.89	76.56
20	69.55	79.4	69.20	69.20	73.98	76.40
21	69.69	78.8	68.84	70.37	76.52	79.90
22	70.22	79.8	69.90	70.37	74.58	76.92
23	70.37	80.6	70.04	70.43	74.58	77.55
24	70.08	80.7	69.60	69.95	74.80	77.90
25	70.05	79.9	69.73	70.65	79.23	83.71
26	71.67	88.0	71.73	71.95	76.40	78.35
27	71.44	87.6	71.17	71.64	75.47	77.18
28	71.17	89.4	71.37	71.37	75.25	76.97
29	71.01	91.0	71.04	71.27	75.06	76.61
30	70.90	92.5	70.84	71.45	74.80	77.23
31	70.75	93.2	70.84	71.22	75.06	77.01
32	71.53	96.0	71.55	72.39	77.23	79.66
33	71.99	92.0	71.95	72.52	78.07	80.79
34	71.95	93.4	72.16	73.19	78.91	82.47
20-1	69.47	78.6	68.59	69.11	71.77	73.05
2	69.58	79.9	68.84	69.39	73.48	75.38
3	69.53	79.9	68.80	69.51	74.58	77.99
4	70.22	77.7	69.25	69.30	74.36	76.52
5	69.98	78.4	68.59	69.07	73.05	74.89
6	69.98	75.3	70.05	68.31	71.82	74.36
7	70.04	78.1	68.50	68.89	72.65	74.50
8	70.39	80.8	68.93	69.47	73.58	75.69
9	70.41	82.1	69.30	69.35	73.80	76.14
10	70.47	78.6	70.43	70.43	74.76	77.23
11	70.53	78.1	70.35	70.60	74.89	77.63
12	70.79	77.7	70.65	70.75	75.34	77.67
13	70.84	78.6	70.60	70.79	75.55	78.21
14	71.10	78.1	70.65	71.00	75.30	78.35
15	71.15	77.5	70.70	71.27	75.81	79.27
16	71.04	77.7	70.84	71.50	75.21	77.18
17	70.92	79.7	71.37	72.82	79.71	85.33
18	72.31	80.3	72.07	72.65	75.90	77.81
19	72.26	81.2	72.16	72.86	76.40	78.21

(1)*	(8)	(9)	(10)	(11)	(12)
5-7	78.91	79.71	84.55	75.90	72.56
8	77.67	78.30	83.85	74.80	72.65
9	76.32	76.80	83.00	73.53	71.86
10	76.52	77.13	85.03	73.44	71.73
11	96.0	98.1	100.3	90.5	83.27
12	77.76	78.11	81.64	76.09	73.32
13	74.54	75.21	78.25	73.28	71.27
14	72.30	72.65	77.99	70.37	69.60
15	72.69	72.82	80.60	70.37	69.51
16	72.82	73.05	81.89	70.35	69.39
17	74.02	73.80	83.23	71.09	70.17
18	73.80	73.98	84.78	70.96	70.25
19	74.45	74.14	87.2	71.45	70.56
20	75.64	76.14	83.00	73.24	71.50
21	79.32	79.99	86.45	76.32	72.82
22	75.47	75.73	85.57	72.56	71.27
23	75.25	75.34	89.4	72.02	71.17
24	75.77	75.77	89.8	72.16	71.00
25	83.18	84.32	92.6	79.40	75.25
26	77.81	78.11	86.10	74.85	73.53
27	76.24	76.56	84.55	73.75	72.60
28	75.86	76.00	85.03	73.28	72.16
29	75.69	76.32	86.45	72.82	71.95
30	75.77	76.05	87.00	72.69	71.60
31	75.51	75.73	88.9	72.20	71.13
32	78.56	79.18	85.92	75.69	73.70
33	80.47	81.36	87.3	77.23	74.63
34	82.59	83.80	87.7	79.27	76.40
20-1	72.56	72.86	76.56	71.04	69.73
2	75.02	75.47	79.14	73.28	70.96
3	77.67	78.30	81.93	75.47	72.25
4	75.47	75.77	82.85	72.82	70.96
5	73.93	74.28	81.18	71.41	70.17
6	73.58	74.10	80.38	70.79	69.81
7	73.48	73.70	81.93	70.84	69.73
8	74.36	74.36	83.94	71.27	70.08
9	74.63	74.63	86.54	71.41	69.99
10	75.47	75.47	86.54	72.39	71.68
11	75.90	76.00	88.4	72.60	71.73
12	76.14	76.32	89.8	73.05	72.16
13	76.52	76.56	90.2	73.28	72.12
14	76.19	76.35	90.0	72.91	72.20
15	76.97	77.05	92.4	73.28	72.25
16	76.00	76.24	84.86	73.32	72.20
17	85.92	86.53	89.6	81.89	77.90
18	76.43	76.61	85.79	74.02	72.90
19	77.05	77.23	86.32	74.28	73.10

(1)*	(13)	(14)	(15)	(16)	(17)
5-7	44		33		1959
8	146	7	120	5	1139
9	295	14	231	10	1296
10	571	28	424	19	1646
11	6				547
12	18		12		544
13	47	2	36	2	594
14	597	28	435	19	996
15		61		39	1500
16		75		45	1736
17		120		67	1879
18		193		107	2175
19		301		158	2581
20	329	16	257	13	1356
21	89	4	74	5	1130
22		88		53	1932
23		387		194	2720
24		212		191	2720
25	82	5	64		1594
26	332	16	259	12	1280
27	654	30	472	23	1278
28		60		41	1513
29		118		68	1797
30		203		115	2034
31		387		202	2435
32	202	10	165	9	1148
33	90	4	80	5	1026
34	31		30		766
20-1	390	18	337	14	726
2	127	6	129	6	726
3	69	3	67	3	726
4	556	26	456	20	1385
5		44		33	1385
6		63		46	1385
7		83		68	1579
8		105		70	1901
9		147		94	2272
10		191		118	2272
11		213		130	2525
12		242		144	2796
13		285		167	2882
14		320		185	2886
15		383		217	3360
16		103		71	1784
17	23		27		685
18		170		107	1872
19		125		83	1872

(1)*	(2)	(3)	(4)	(5)	(6)	(7)
20-20	72.34	79.9	72.25	73.10	77.90	79.90
21	72.28	80.3	71.99	72.82	76.24	78.21
22	72.23	79.9	71.90	73.15	76.80	78.21
23	71.72	86.3	71.33	71.50	75.47	76.97
24	71.35	87.3	70.96	71.13	75.02	76.52
25	71.13	86.5	70.60	71.04	74.58	76.09
26	70.77	86.8	70.48	70.79	74.85	76.48
27	71.00	88.1	70.56	70.84	74.40	75.51
28	71.32	87.0	70.60	71.04	75.47	77.67
29	71.29	88.0	70.52	71.04	75.34	77.94
35-1	71.06	85.7	70.92	71.41	76.14	78.35
2	71.35	87.0	71.37	71.68	76.65	78.52
3	71.27	88.8	71.50	71.68	76.43	77.86
4	70.92	88.4	70.75	71.04	75.69	77.81
5	73.30	87.6	73.36	73.36	78.07	81.05
6	73.45	88.0	73.48	73.80	78.56	81.45
7	73.53	90.1	73.58	74.10	77.76	80.84
8	73.54	86.8	73.70	73.70	78.03	80.65
9	73.83	83.2	73.28	73.62	78.56	81.27
10	73.98	80.3	73.48	73.89	78.48	81.14
11	74.03	84.4	72.82	74.19	78.11	80.75
12	73.99	85.7	73.36	73.53	77.81	79.99
13	74.44	84.3	73.93	74.80	80.84	83.80
14	73.67	83.7	72.86	74.23	80.21	83.00
15	73.00	85.0	72.86	73.70	79.66	83.75
16	73.92	85.7	73.70	74.50	79.00	83.27
17	69.16	85.0	69.30	69.73	73.98	78.35
18	68.94	87.6	68.84	69.95	74.89	80.70
19	69.40	88.1	69.35	69.99	72.25	75.25
20	69.37	88.4	69.07	69.73	72.44	74.10
50-1	68.88	76.8	69.07	69.35	76.14	80.12
2	68.86	79.9	69.07	69.07	75.25	78.56
3	68.80	79.9	68.80	69.30	74.76	77.59
4	68.90	80.6	69.02	69.30	75.38	78.16
5	68.84	80.3	68.93	69.43	75.25	77.90
6	69.06	83.0	68.84	69.69	75.34	77.72
7	69.06	80.8	68.80	68.64	74.54	78.56
8	69.42	84.3	69.77	69.95	75.47	77.94
9	71.44	82.6	71.41	71.55	75.38	77.36
10	71.16	80.3	70.84	71.22	78.11	82.29
11	71.22	83.4	70.84	71.60	77.86	82.29
12	71.29	84.8	71.00	71.73	77.50	83.53
13	70.52	85.7	71.04	71.50	77.09	82.34
14	70.58	85.7	71.00	71.86	77.32	84.41
15	70.52	80.8	70.21	71.50	77.09	83.89
16	70.29	82.1	70.12	70.84	75.51	82.06
17	70.57	85.0	70.60	71.99	75.42	80.33
18	71.56	81.8	71.13	71.73	75.73	77.94
19	71.44	77.7	70.84	71.33	75.77	77.59

(1)*	(8)	(9)	(10)	(11)	(12)
20-20	78.65	79.00	87.10	75.69	74.02
21	77.32	77.50	85.21	74.58	73.28
22	77.67	78.03	83.67	76.09	74.19
23	76.43	77.05	83.00	73.98	72.73
24	75.90	76.19	83.05	73.32	72.20
25	75.51	75.86	82.77	72.79	71.73
26	75.51	75.51	87.8	71.99	71.17
27	75.21	75.69	79.76	73.58	71.73
28	77.50	78.25	82.10	74.54	72.69
29	77.81	78.11	81.72	75.02	73.05
35-1	77.76	77.76	87.1	73.84	72.60
2	77.90	77.67	86.45	74.50	72.78
3	77.45	77.45	86.75	73.70	72.16
4	76.80	76.85	89.8	73.15	71.55
5	79.49	79.66	88.5	75.77	74.36
6	79.81	79.99	90.2	75.69	74.50
7	79.27	79.95	89.8	75.69	74.40
8	79.00	79.40	89.5	75.47	74.40
9	79.53	79.76	89.7	75.69	74.63
10	79.49	79.66	89.0	75.64	74.63
11	78.85	79.14	88.7	75.51	74.58
12	79.36	79.44	88.9	75.25	74.68
13	83.00	83.80	88.4	78.56	76.35
14	82.29	83.00	89.1	77.86	74.76
15	83.23	83.80	87.5	79.32	75.77
16	82.81	83.23	86.10	78.96	76.52
17	78.83	79.66	81.40	75.60	73.24
18	81.10	82.38	84.95	78.03	75.42
19	75.42	75.81	76.48	73.65	71.86
20	73.70	74.40	76.56	71.90	70.17
50-1	79.40	79.95	87.4	74.80	71.37
2	77.90	78.07	85.35	73.65	70.70
3	77.01	77.13	84.69	72.65	70.48
4	77.45	77.76	85.65	72.86	70.37
5	76.61	77.05	85.65	72.39	70.37
6	76.70	77.13	86.75	72.20	70.37
7	77.55	77.86	89.1	72.65	70.17
8	76.61	76.80	87.8	72.39	70.52
9	76.24	76.61	85.48	73.48	72.16
10	81.72	82.10	87.4	77.27	73.98
11	81.36	82.29	87.0	77.32	74.14
12	82.90	83.14	87.8	78.60	75.02
13	83.00	83.18	86.9	78.35	75.25
14	83.80	83.89	87.8	79.90	75.90
15	82.95	82.85	86.2	79.32	76.14
16	82.29	82.34	84.11	78.48	76.43
17	81.01	81.27	82.85	77.63	75.55
18	76.75	76.97	86.62	73.36	72.39
19	75.90	76.80	86.31	73.05	72.16

(1)*	(13)	(14)	(15)	(16)	(17)
20-20		36		282	1621
21		73		52	1613
22	390	19	349	17	1125
23	423	19	340	17	1012
24	680	32	546	25	1191
25		54		40	1264
26		213		129	2208
27	229	11	208	10	700
28	109		98		697
29	65		64		573
35-1		45		38	1269
2		44		38	1339
3		65		48	1320
4		82		58	1580
5		107		82	1808
6		145		106	2128
7		192		134	2128
8		211		148	2164
9		239		165	2273
10		289		188	2273
11		319		207	2273
12		392		241	2273
13	410	19	380	17	1126
14	557	26	536	23	1275
15	169	8	116	4	777
16	84	4	102	3	513
17	91	5	75	4	390
18	59	3	36		390
19	78	4	57	2	153
20	232	11	227	10	387
50-1		44		50	1273
2		57		63	1268
3		69		73	1255
4		85		85	1494
5		110		103	1575
6		139		125	1824
7		157		139	1977
8		212		177	2028
9		243		197	1662
10		30		36	1000
11	558	26	683	32	939
12	410	20	517	24	847
13	307	14	384	18	715
14	219	10	261	12	595
15	161		211		455
16	118		172		401
17	71		126		308
18		297		236	1737
19		331		260	1737

(1)*	(2)	(3)	(4)	(5)	(6)	(7)
S-1	73.90	89.3	73.89	74.68	81.10	83.44
2	72.86	89.2	72.65	73.48	78.48	80.07
3	73.09	88.9	72.60	73.48	79.23	80.97
4	70.58	80.4	70.48	71.00	76.61	78.35
5	70.68	80.6	70.70	71.04	76.56	78.11
6	70.41	81.0	70.52	70.84	76.56	77.99
7	70.90	79.7	70.37	71.00	75.11	76.56
8	70.81	84.9	70.60	71.95	76.14	77.99
9	70.93	81.8	70.65	71.27	75.34	77.36
10	71.08	80.1	70.88	71.90	76.48	79.18
11	71.46	80.3	71.27	71.99	75.21	77.18
12	71.42	77.7	71.13	71.82	74.68	76.56

(1)*	(8)	(9)	(10)	(11)	(12)
S-1	82.85	83.27	88.9	77.81	75.69
2	79.44	80.17	86.15	75.69	73.93
3	80.38	80.70	87.1	75.73	74.40
4	77.50	77.81	85.57	73.28	71.77
5	77.13	77.36	85.92	73.15	71.50
6	76.97	77.36	85.65	72.82	71.17
7	76.52	77.50	79.90	73.93	71.82
8	78.03	78.44	80.79	74.40	72.12
9	77.27	77.86	79.90	74.28	72.39
10	79.10	79.90	81.22	75.47	73.15
11	77.67	77.81	78.70	74.72	73.10
12	77.01	77.59	77.76	74.58	73.19

(1)*	(13)	(14)	(15)	(16)	(17)
S-1		50		35	991
2		96		59	991
3		130		75	1186
4		231		125	1270
5		399		200	1415
6		343		178	1360
7	578	38	433	21	462
8	369	17	294	14	473
9	243	12	200		386
10	131	7	126		386
11	58		74		205
12	23		44		139

TABLE 5

Calculated Data

(1) Run No.	(2) w, lb_m sec	(3) Average t_b, °F	(4) Average t_w, °F	(5) Driving Force (t_w-t_b)	(6) Temp. Rise $(t_{b_2}-t_{b_1})$
W-1	0.528	72.35	77.16	4.81	1.737
2	0.455	71.44	76.43	4.79	2.052
3	0.628	70.97	77.28	6.31	2.133
4	1.66	71.13	75.32	4.19	0.999
5	2.35	72.01	76.44	4.43	0.882
6	1.05	72.17	76.91	4.74	1.377
7	0.88	71.91	75.45	3.54	1.188
8	2.13	71.39	74.53	3.14	0.690
9	1.13	70.21	73.68	3.47	1.179
10	2.84	70.57	73.58	3.01	0.963
11	0.115	71.76	82.59	10.83	6.084
12	0.192	70.63	76.21	5.58	3.132
13	0.266	70.90	74.35	3.45	2.313
14	0.62	72.32	78.19	5.87	2.133
15	2.25	70.48	74.03	3.55	0.711
16	1.59	71.15	74.83	3.68	0.972
17	1.359	71.32	75.50	4.18	1.134
18	0.180	70.01	74.31	4.30	2.718
19	2.72	71.50	76.57	5.07	0.963
20	0.231	71.51	82.21	10.70	4.730
21	0.260	74.21	83.24	9.03	4.131
22	2.92	73.27	77.66	4.37	0.963
23	0.88	70.95	74.86	3.91	1.170
24	1.295	70.30	74.08	3.78	0.927
25	2.40	70.14	74.23	4.09	0.738
26	3.27	70.27	74.37	4.10	0.630
27	0.343	71.92	78.44	6.52	2.664
5-1	1.08	71.09	74.52	3.69	1.530
2	2.14	70.73	73.23	2.76	0.963
3	2.59	70.64	72.57	2.19	0.810
4	2.93	71.49	73.87	2.64	0.918
5	0.645	71.35	74.31	3.22	1.854
6	0.343	72.28	77.68	5.66	3.276
7	0.240	71.37	77.59	6.48	3.465
8	0.435	71.27	76.72	5.71	2.286
9	0.610	70.68	75.50	5.08	1.872
10	0.855	70.71	75.84	5.39	1.674
11		72.04	90.37	18.59	7.281

Table 5 - continued

Calculated Data

(1) Run No.	(7) St x 10^3	(8) f x 10^3	(9) μ, centipoise	(10) Re x 10^3	(11) $St(C_p)^{2/3}$ x 10^3
W-1	0.934	6.690	0.949	17.03	1.63
2	1.064	6.404	0.960	14.51	1.87
3	0.874	7.036	0.966	19.79	1.54
4	0.617	5.227	0.964	52.66	1.08
5	0.515	4.421	0.953	74.94	0.90
6	0.752	5.758	0.951	33.78	1.31
7	0.868	5.223	0.954	28.21	1.52
8	0.568	4.735	0.961	67.75	1.00
9	0.879	5.763	0.976	35.41	1.56
10	0.828	4.480	0.971	89.40	1.46
11	1.453	8.495	0.956	3.71	2.54
12	1.452	7.314	0.970	6.07	2.56
13	1.734	6.669	0.967	8.43	3.06
14	0.940	6.459	0.947	20.00	1.64
15	0.518	4.726	0.972	70.71	0.92
16	0.683	5.311	0.964	50.44	1.20
17	0.702	5.288	0.961	43.22	1.23
18	1.635	5.184	0.978	5.65	2.90
19	0.491	4.389	0.959	86.65	0.86
20	1.144	6.527	0.959	7.41	2.01
21	1.183	7.146	0.926	8.62	2.03
22	0.567	4.381	0.937	95.20	0.98
23	0.778	6.107	0.966	27.80	1.37
24	0.638	5.678	0.975	40.53	1.13
25	0.469	4.662	0.977	75.00	0.83
26	0.400	4.658	0.975	102.35	0.71
27	1.062	6.677	0.954	10.98	1.85
5-1	1.073	6.057	1.235	26.69	
2	0.903	4.893	1.138	57.39	
3	0.957	4.721	1.101	71.79	
4	0.900	4.540	1.076	83.10	
5	1.490	6.857	1.255	15.68	
6	1.497	7.338	1.255	8.34	3.10
7	1.383	6.425	1.255	5.84	2.87
8	1.036	7.036	1.255	10.58	2.14
9	0.953	6.900	1.255	14.83	1.98
10	0.803	6.440	1.250	20.87	1.66
11	1.013				

Table 5 - Continued

Calculated Data

(1) Run No.	(12) $St(P_r)^{2/3} \times 10^3$	(13) h, Btu/(hr)(ft^2)(°F)	(14) $q = wC_p \Delta t_b$, watts	(15) $1/\sqrt{f}$	(16) $w\sqrt{f}$
W-1	3.30	586	968	12.23	0.043
2	3.79	575	985	12.50	0.036
3	3.13	652	1413	11.92	0.053
4	2.19	1220	1750	13.83	0.120
5	1.82	1438	2187	15.04	0.156
6	2.66	938	1525	13.18	0.080
7	3.08	907	1103	13.84	0.064
8	2.02	1437	1551	14.53	0.147
9	3.17	1180	1406	13.17	0.086
10	2.97	2794	2885	14.94	0.190
11	5.16	199	738	10.85	0.011
12	5.21	331	634	11.69	0.016
13	6.21	548	649	12.25	0.022
14	3.32	692	1395	12.44	0.050
15	1.86	1385	1688	14.55	0.155
16	2.44	1290	1630	13.72	0.116
17	2.50	1133	1626	13.75	0.099
18	5.89	350	516	13.89	0.013
19	1.75	1587	2763	15.09	0.180
20	4.07	314	1153	12.38	0.019
21	4.12	365	1133	11.83	0.022
22	1.99	1967	2967	15.11	0.193
23	2.78	813	1086	12.80	0.069
24	2.30	982	1266	13.27	0.098
25	1.69	1337	1869	14.65	0.164
26	1.44	1554	2173	14.65	0.223
27	3.76	433	964	12.24	0.028
5-1		1349	1582	12.85	0.084
2		2250	2131	14.29	0.150
3		2885	2169	14.55	0.178
4		3069	2781	14.84	0.198
5		1119	1237	12.08	0.053
6		598	1161	11.67	0.029
7		386	859	12.48	0.019
8	4.25	525	1028	11.92	0.037
9	3.92	677	1181	12.04	0.051
10	3.30	1565	1480	12.46	0.069
11					

(1)	(2)	(3)	(4)	(5)	(6)
5-12	0.157	70.37	76.39	6.28	3.141
13	0.247	69.75	73.80	4.31	2.106
14	0.875	69.25	71.92	2.93	1.143
15	1.30	69.45	72.35	3.16	1.071
16	1.43	70.20	72.40	2.20	2.898
17	1.82	69.39	73.49	4.36	0.972
18	2.31	69.48	73.39	4.17	0.900
19	2.80	69.88	74.13	4.51	0.855
20	0.650	70.25	74.95	4.76	1.827
21	0.338	70.80	78.30	7.76	2.907
22	1.56	70.66	75.00	4.60	1.152
23	3.27	70.69	74.82	4.39	0.846
24	2.41	70.50	75.27	5.03	1.098
25	0.327	71.67	81.81	10.30	4.257
26	0.650	72.35	77.40	5.05	1.773
27	0.910	71.92	76.04	4.12	1.269
28	1.295	71.59	75.68	4.09	1.089
29	1.80	71.37	75.59	4.22	0.945
30	2.38	71.21	75.50	4.29	0.819
31	3.27	71.03	75.40	4.37	0.738
32	0.505	72.31	78.23	5.92	2.043
33	0.350	73.03	79.83	6.80	2.718
34	0.202	73.32	81.59	8.27	3.582
20-1	0.695	69.84	72.12	2.54	0.972
2	0.403	70.20	74.38	4.44	1.629
3	0.303	70.47	76.54	6.33	2.475
4	0.825	70.84	74.95	4.37	1.620
5	1.09	70.45	73.47	3.28	1.233
6	1.30	70.38	72.86	2.74	1.053
7	1.49	70.44	73.05	2.87	1.062
8	1.69	70.83	73.89	3.32	1.152
9	1.98	70.85	74.16	3.51	1.143
10	2.25	70.86	75.02	4.42	1.017
11	2.39	70.93	75.40	4.73	1.044
12	2.53	71.21	75.67	4.72	1.089
13	2.74	71.23	76.00	5.03	1.035
14	2.92	71.47	75.69	4.48	0.981
15	3.20	71.55	76.40	5.11	1.053
16	1.66	71.45	75.56	4.37	1.071
17	0.199	72.39	83.98	11.59	3.861
18	2.12	72.65	76.09	3.70	0.882
19	1.83	72.64	76.65	4.27	0.990
20	0.98	72.93	78.23	5.56	1.537
21	1.39	72.60	76.75	4.41	1.134
22	0.695	72.82	77.24	4.68	1.557
23	0.72	72.25	76.22	3.97	1.386

(1)	(7)	(8)	(9)	(10)	(11)
5-12	1.294	5.459	1.255	3.82	2.68
13	1.264	6.615	1.255	6.00	2.62
14	1.009	6.370	1.249	21.38	2.09
15	0.877	5.622	1.214	32.68	1.77
16	0.902	5.361	1.202	36.31	1.81
17	0.577	4.927	1.166	47.63	1.14
18	0.558	4.885	1.124	62.72	1.07
19	0.490	4.910	1.085	78.75	0.92
20	0.953	6.820	1.255	15.81	1.97
21	0.969	7.266	1.255	8.22	2.01
22	0.648	5.306	1.190	40.01	1.30
23	0.499	4.419	1.053	94.77	0.92
24	0.565	4.991	1.115	65.96	1.08
25	1.069	6.710	1.255	7.95	2.22
26	0.908	6.873	1.255	15.81	1.88
27	0.797	6.390	1.247	22.27	1.65
28	0.680	5.956	1.215	32.53	1.40
29	0.579	5.113	1.168	47.03	1.14
30	0.494	4.946	1.127	64.45	0.95
31	0.437	4.602	1.053	94.77	0.81
32	0.893	7.253	1.255	12.28	1.85
33	1.034	7.317	1.255	8.51	2.14
34	1.121	8.259	1.255	4.91	2.32
20-1	0.990	7.455	1.952	10.87	2.64
2	0.949	8.543	2.013	6.11	2.58
3	1.012	7.834	2.033	4.55	2.76
4	0.959		1.925	13.08	2.53
5	0.973	6.487	1.869	17.80	2.51
6	0.994	6.357	1.822	21.77	2.53
7	0.957	7.153	1.783	25.50	2.40
8	0.898	5.724	1.743	29.59	2.21
9	0.828	5.600	1.687	35.82	2.00
10	0.595	5.444	1.639	41.89	2.22
11	0.571	5.315	1.612	45.25	1.34
12	0.597	5.254	1.590	48.56	1.38
13	0.532	5.195	1.556	53.74	1.22
14	0.567	5.067	1.530	58.24	1.28
15	0.533	4.949	1.496	65.28	1.19
16	0.634	6.017	1.750	28.90	1.57
17	0.862	7.328	2.055	2.96	2.37
18	0.617	5.560	1.660	38.97	1.47
19	0.600	5.789	1.716	32.54	1.46
20	0.715	6.809	1.890	15.82	1.86
21	0.665	6.286	1.803	23.53	1.68
22	0.861	7.765	1.952	10.87	2.29
23	0.903	7.253	1.946	11.29	2.43

(1)	(12)	(13)	(14)	(15)	(16)
5-12	5.32	236	510	13.54	0.012
13	5.20	363	538	12.30	0.020
14	4.14	1028	1034	12.53	0.070
15	3.52	1327	1440	13.34	0.098
16	3.60	1502	1623	13.66	0.105
17	2.26	1222	1829	14.25	0.128
18	2.13	1500	2149	14.31	0.162
19	1.83	1597	2475	14.27	0.196
20	3.91	721	1228	12.11	0.054
21	3.98	381	1016	11.73	0.029
22	2.58	1177	1858	13.73	0.114
23	1.82	1900	2861	15.04	0.217
24	2.15	1585	2736	14.16	0.170
25	4.40	407	1439	12.20	0.027
26	3.73	688	1192	12.06	0.054
27	3.27	845	1194	12.51	0.073
28	2.78	1040	1458	12.96	0.100
29	2.27	1214	1759	13.99	0.129
30	1.89	1370	2015	14.22	0.167
31	1.60	1665	2495	14.74	0.222
32	3.67	526	1067	11.74	0.043
33	4.25	422	984	11.69	0.030
34	4.61	264	748	11.00	0.018
20-1	5.23	748	653	11.58	0.060
2	5.12	416	634	10.82	0.037
3	5.47	333	724	11.30	0.027
4	5.01	860	1291		
5	4.98	1153	1298	12.32	0.089
6	5.01	1406	1322	12.54	0.104
7	4.75	1551	1528	11.82	0.126
8	4.38	1650	1880	13.22	0.128
9	3.96	1784	2186	13.37	0.148
10	4.40	1457	2210	13.55	0.166
11	2.65	2048	2410	13.72	0.174
12	2.74	1642	2661	13.79	0.183
13	2.41	1586	2739	13.87	0.198
14	2.54	1799	2767	14.05	0.208
15	2.36	1855	3255	14.23	0.225
16	3.10	1145	1717	12.88	0.129
17	4.70	187	742	11.68	0.017
18	2.92	1422	1806	13.39	0.158
19	2.90	1194	1750	13.14	0.139
20	3.69	762	1455	12.12	0.081
21	3.33	1006	1523	12.61	0.110
22	4.54	650	1045	11.35	0.061
23	4.82	723	985	11.74	0.061

(1)	(2)	(3)	(4)	(5)	(6)
20-24	0.91	71.83	75.66	3.83	1.251
25	1.20	71.53	75.26	3.73	1.053
26	2.39	71.13	75.29	4.16	0.945
27	0.554	71.48	75.03	3.55	1.260
28	0.375	72.03	76.96	4.93	1.854
29	0.294	72.04	77.05	5.01	1.971
30-1	1.08	71.53	77.23	5.70	1.233
2	1.07	71.84	77.45	5.61	1.287
3	1.29	71.76	77.11	5.35	1.080
4	1.46	71.37	76.44	5.07	1.179
5	1.65	73.73	79.05	5.32	1.134
6	1.93	73.90	79.43	5.53	1.170
7	2.21	73.91	78.89	4.98	0.999
8	2.32	73.91	78.75	4.84	0.981
9	2.49	74.20	79.25	5.05	0.981
10	2.73	74.32	79.19	4.87	0.891
11	2.86	74.36	78.66	4.30	0.855
12	3.09	74.30	78.86	4.56	0.801
13	0.70	75.05	82.43	7.38	1.611
14	0.818	74.24	81.73	7.49	1.503
15	0.46	73.71	82.15	8.44	1.872
16	0.333	74.50	81.63	7.13	1.521
17	0.276	69.77	76.08	6.31	1.602
18	0.082	70.08	79.28	9.20	2.988
19	0.223	69.77	74.44	4.67	0.972
20	0.521	69.70	73.41	3.71	0.855
50-1	1.05	69.40	78.42	9.02	1.377
2	1.20	69.32	77.06	7.74	1.206
3	1.30	69.23	76.29	7.06	1.116
4	1.455	69.36	76.78	7.42	1.197
5	1.65	69.28	76.24	6.96	1.152
6	1.85	69.50	76.33	6.83	1.161
7	1.985	69.52	76.61	7.09	1.197
8	2.39	69.82	76.27	6.45	1.062
9	2.46	71.76	76.02	4.26	0.828
10	0.865	71.65	80.60	8.95	1.296
11	0.81	71.70	80.37	8.67	1.269
12	0.734	71.81	81.17	9.36	1.359
13	0.635	71.01	81.09	10.08	1.287
14	0.536	71.07	81.69	10.62	1.278
15	0.474	70.97	81.01	10.04	1.179
16	0.420	70.74	80.07	9.33	1.170
17	0.332	71.01	79.22	8.21	1.152
18	2.71	71.87	76.45	4.58	0.801
19	2.86	71.73	76.01	4.28	0.765
S-1	1.05	74.53	82.35	7.82	1.656

(1)	(7)	(8)	(9)	(10)	(11)
20-24	0.845	7.082	1.905	14.58	2.24
25	0.730	6.486	1.843	19.87	1.90
26	0.588	5.274	1.612	45.25	1.39
27	0.918	7.290	1.981	8.54	2.50
28	0.973	7.498	2.020	5.66	2.69
29	1.018	7.959	2.035	4.41	2.82
35-1	0.560	7.350	3.19	10.33	1.96
2	0.593	7.488	3.20	10.20	2.08
3	0.522	6.508	3.11	12.66	1.80
4	0.602	6.138	3.04	14.66	2.04
5	0.551	6.795	2.97	16.95	1.84
6	0.547	6.420	2.87	20.52	1.78
7	0.519	6.190	2.78	24.26	1.65
8	0.524	6.203	2.75	25.75	1.66
9	0.503	6.004	2.70	28.14	1.57
10	0.473	5.691	2.63	31.68	1.46
11	0.514	5.709	2.60	33.57	1.57
12	0.454	5.694	2.55	36.98	1.37
13	0.565	8.051	3.30	6.47	2.02
14	0.519	8.317	3.28	7.62	1.85
15	0.572	5.691	3.33	4.22	2.06
16	0.552	9.550	3.33	3.05	1.99
17	0.657	10.259	3.34	2.52	2.37
18	0.840		3.35	0.75	3.04
19	0.539	11.900	3.34	2.04	1.94
20	0.596	8.689	3.32	4.79	2.14
50-1	0.395	9.872	7.54	4.25	2.30
2	0.403	9.524	7.29	5.02	2.30
3	0.409	9.403	7.11	5.58	2.29
4	0.417	8.740	6.87	6.46	2.26
5	0.428	8.236	6.53	7.71	2.26
6	0.440	7.951	6.24	9.05	2.26
7	0.437	7.680	6.05	10.01	2.20
8	0.426	6.746	5.28	13.81	1.96
9	0.503	7.087	5.41	13.87	2.36
10	0.375	10.474	7.88	3.35	2.25
11	0.379	10.306	7.97	3.10	2.28
12	0.376	9.608	8.10	2.77	2.29
13	0.330	9.555	8.29	2.34	2.05
14	0.311	9.094	8.45	1.94	1.96
15	0.304	9.412	8.55	1.69	1.92
16	0.325	9.759	8.66	1.48	2.08
17	0.363	11.42	8.83	1.15	2.36
18	0.452	6.996	5.14	16.09	2.89
19	0.462	6.920	5.00	17.46	2.05
S-1	0.548	6.073	0.946	33.86	0.574

(1)	(12)	(13)	(14)	(15)	(16)
20-24	4.44	855	1124	11.88	0.077
25	3.76	974	1248	12.42	0.097
26	2.76	1561	2230	13.77	0.174
27	4.96	566	689	11.71	0.047
28	5.32	405	686	11.55	0.033
29	5.59	333	572	11.21	0.026
35-1	3.89	607	1188	11.67	0.093
2	4.12	638	1229	11.56	0.093
3	3.56	677	1243	12.40	0.104
4	4.05	883	1536	12.76	0.114
5	3.65	914	1670	12.13	0.136
6	3.54	1062	2015	12.48	0.155
7	3.28	1152	1970	12.71	0.174
8	3.29	1222	2031	12.70	0.183
9	3.12	1257	2180	12.91	0.193
10	2.89	1298	2171	13.26	0.206
11	3.11	1479	2182	13.24	0.216
12	2.72	1411	2209	13.25	0.233
13	4.00	397	1006	11.15	0.063
14	3.66	427	1097	10.97	0.075
15	4.08	264	768	13.26	0.035
16	3.94	185	452	10.23	0.033
17	4.70	182	395	9.87	0.028
18	6.03	69	219	4.24	0.019
19	3.85	121	193	9.17	0.024
20	4.23	312	398	10.73	0.049
50-1	4.58	379	1175	10.06	0.104
2	4.57	443	1176	10.25	0.117
3	4.55	486	1179	10.31	0.126
4	4.49	555	1415	10.70	0.136
5	4.49	646	1545	11.02	0.150
6	4.49	744	1745	11.21	0.165
7	4.37	793	1931	11.42	0.174
8	3.90	931	2063	12.18	0.196
9	4.68	1131	1655	11.88	0.207
10	4.46	296	911	9.78	0.089
11	4.53	281	835	9.85	0.082
12	4.55	252	811	10.20	0.072
13	4.06	192	664	10.23	0.062
14	3.89	153	557	10.48	0.051
15	3.82	132	454	10.31	0.046
16	4.13	125	399	10.12	0.042
17	4.69	110	311	9.36	0.036
18	5.74	1121	1764	11.96	0.227
19	4.07	1210	1778	12.02	0.238
S-1	2.63	320	858	12.82	0.082

(1)	(2)	(3)	(4)	(5)	(6)
S-2	1.46	73.32	79.25	5.93	1.215
3	1.69	73.53	80.06	6.53	1.143
4	2.25	70.99	77.26	6.27	1.071
5	2.96	71.04	76.98	5.94	0.954
6	2.73	70.79	76.90	6.11	0.990
7	0.78	71.33	76.22	4.89	1.116
8	0.628	71.32	77.48	6.16	1.350
9	0.524	71.45	76.74	5.29	1.377
10	0.414	71.75	78.38	6.63	1.746
11	0.318	71.99	76.89	4.90	1.386
12	0.252	71.92	76.34	4.42	1.314

(1)	(7)	(8)	(9)	(10)	(11)
S-2	0.530	5.295	0.946	47.08	0.555
3	0.453	5.023	0.946	54.50	0.474
4	0.442	4.723	0.946	72.56	0.463
5	0.416	4.366	0.946	95.46	0.435
6	0.419	4.568	0.946	88.04	0.439
7	0.590	6.264	0.946	25.15	0.618
8	0.567	6.561	0.946	20.25	0.594
9	0.673	6.410	0.946	16.90	0.705
10	0.681	6.482	0.946	13.34	0.713
11	0.732	6.437	0.946	10.26	0.766
12	0.769	6.084	0.946	8.14	0.805

(1)	(12)	(13)	(14)	(15)	(16)
S-2	2.55	430	875	13.73	0.106
3	2.17	425	953	14.12	0.120
4	2.12	552	1189	14.53	0.155
5	2.00	683	1393	15.11	0.196
6	2.01	636	1333	14.79	0.185
7	2.83	256	429	12.61	0.062
8	2.72	198	418	12.33	0.051
9	3.23	196	356	12.48	0.042
10	3.27	157	357	12.42	0.033
11	3.51	129	217	12.47	0.026
12	3.69	108	163	12.81	0.020